Extended rays and wave energy flux in complex geometrical optics

Omar Maj,[1, a)] Alberto Mariani,[2] Emanuele Poli,[1] and Daniela Farina[2]
[1)] *Max Planck Institute for Plasma Physics, EURATOM Association, Boltzmannstr. 2, 85748 Garching, Germany.*
[2)] *Istituto di Fisica del Plasma "P. Caldirola", Consiglio Nazionale delle Ricerche, EURATOM-ENEA-CNR Association, via R. Cozzi 53, I-20125 Milano, Italy.*

The description of high-frequency beams in inhomogeneous dispersive media is usually dealt with by asymptotic methods that greatly simplify the computational problem. This is the case of electron cyclotron heating and current drive applications in large magnetic confinement devices, where the wave-length to plasma-size ratio is extremely small, thus, hampering the direct numerical solution of the relevant wave equation. One such method is complex geometrical optics in its eikonal-based formulation. The theoretical basis of this method, however, appears to have received relatively less consideration, so that many important aspects, such as wave energy transport, have yet to be rigorously clarified. In this work, we attempt to fill up this gap. A precise asymptotic expansion exploiting the paraxial character of complex eikonal waves is proposed, which eventually leads to an equation for the description of the wave energy transport, including the effects of diffraction. The eikonal-based formulation of complex geometrical optics provides the theoretical basis of the `GRAY` code [Farina, Fusion Sci. Technol. **52**, 154 (2007)], which is extensively used in fusion applications. A few numerical experiments are presented, showing, in particular, that extended rays determined by `GRAY` accurately represent the wave energy flow, and that the same information can also be retrieved from the beam tracing code `TORBEAM` [Poli at al., Comp. Phys. Comm. **136**, 90 (2001)].

I. INTRODUCTION

Among the methods employed for the description of wave beams in magnetic confinement devices, the version of the complex geometrical optics method implemented in the `GRAY` code[1] has gained interest in the last few years, and, together with the beam tracing code `TORBEAM`[2], constitutes a major tool for the design of electron cyclotron heating and current drive systems[3].

Complex geometrical optics, rather than to a unified theory, refers to a family of closely related methods for the construction of a uniform asymptotic solution of wave equations in the high-frequency limit, capturing wave effects, such as diffraction. It is a development of high-frequency diffraction theory[4], and, as such, it builds on and extends the standard geometrical optics method. (Among the vast literature available on standard geometrical optics, one can refer to the monograph by Kravtsov and Orlov[5] for a physics overview, to the review paper by McDonald[6] for more insights on operators and symbol calculus, and to Rauch's lectures[7] for mathematically rigorous results, with emphasis on symmetric hyperbolic systems.)

In addition to the variety of complex geometrical optics flavors, other methods, such as the paraxial WKB method developed by Pereverzev[8,9], the complex WKB method[10], and the theory of Gaussian beams[11–13], are deeply related to the techniques and ideas of complex geometrical optics[14,15].

An attempt to a systematic classification of such various aspects of complex geometrical optics has been made in the recent monograph by Kravtsov[16], which includes a comprehensive list of references and a brief historical account; cf. also Červený[17] and references therein. Concerning plasma physics applications, one might distinguish two main branches.

The first branch is complex ray theory, also known as ray-based complex geometrical optics, which relies on the complexification of standard geometrical optics rays (cf. the review papers by Kravtsov et al.[18], Thomson[19], and Chapman et al.[20], as well as the numerical implementations of Egorchenkov and Kravtsov[21] and Amodei et al.[22] and references therein). This has been applied to plasma physics for the description strong damping[23–25], although complex rays can be used to describe diffractive beams as well.

The second branch is the complex eikonal theory[26], also known as eikonal-based complex geometrical optics, which has been applied to fusion-relevant problems by Mazzucato[27], Nowak and Orefice[28–30], Peeters[31], Timofeev[32], and which eventually led to the `GRAY` code[1]. Instead of relying on the complexification of geometrical optics rays, a new set of trajectories in the real space, called extended rays[31], are defined as a perturbation of standard geometrical optics rays due to diffraction.

The rigorous derivation and study of complex rays, however, appears to have received more attention than the eikonal-based counterpart.

In this paper, we review the precise derivation of complex geometrical optics equations in the eikonal-based form, and address, in particular, the issue of the wave energy density flux.

More specifically, a precise asymptotic expansion in high-frequency limit $\kappa = \omega L/c \to +\infty$ is performed, with ω being the frequency of the beam, L the scale length of the medium inhomogeneity, and c the speed of light in free space.

Here, the parameter κ is naturally obtained by a proper

[a)] Electronic mail: omaj@ipp.mpg.de

normalization of the wave equation[9], as opposed to a formal ordering of quantities based on physics arguments. This allows us to perform a precise asymptotic expansion and to take advantage of the paraxial character of the corresponding complex eikonal wave field[9,10], with a significant simplification in the derivation and analysis. The transport equation for the wave energy density is then readily obtained.

This theoretical result is illustrated numerically: the field lines of the wave energy flux vector computed in the `GRAY` code are found to agree with the trajectories of extended rays obtained by `GRAY`, thus, confirming that extended rays represent accurately the energy flow. A comparison is also presented with the field lines of the wave energy flux computed by the beam tracing code `TORBEAM`. Theoretically, the complex eikonal and the beam tracing method should give the same asymptotic solution for a Gaussian beam[31,32], and, thus, the same wave energy flux. This is recovered in the numerical results.

At last, a generalization of the theory to generic dispersive, but weakly dissipative, media is sketched, showing, in particular, the robustness of high-frequency wave asymptotics. Possible applications encompass electrodynamics, elastodynamics, linear waves in fluids and plasmas, as well as quantum mechanics in the semiclassical limit. Our main concern, however, is heating and current drive mechanisms in tokamak plasmas. Therefore, all numerical results refer to electron cyclotron wave beams in tokamak geometry, for which a standard ITER plasma equilibrium is used.

In the presentation of the results, we have tried to account for the vast relevant literature available on high-frequency wave asymptotics, ranging from pure mathematics, to physics applications, particularly, in the field of geophysics, radio-physics, and quantum mechanics. Plasma physics applications are collocated into a broader context of wave theory, and, with this aim, mathematical tools frequently used in the analysis of caustic singularities are reviewed in a simplified way, so that the origin, as well as the limitations, of the complex eikonal approach can be appreciated.

Such background material is reviewed in section II. Specifically, preliminary results on standard geometrical optics are reviewed in section II A, which, in addition, allows us to define the problem and fix the notation. Then, the introduction of a complex phase (eikonal) is justified through the study of a particular caustic geometry (section II B); incidentally, this study shows how geometrical optics rays do encode information on diffraction effects. (This section is self-contained, and it can be safely skipped by a reader who is more interested in the derivation of the equations.) In section III, the main results are reported for the specific case of a spatially non-dispersive medium (such as the cold plasma model), while section IV is devoted to the corresponding numerical results. At last, an approach to the general case of spatially dispersive media is put forward in section V.

II. PRELIMINARY RESULTS

In this section, we fix the notation and review basic results and ideas, upon which the complex geometrical optics method rely.

A. The wave equation and standard geometrical optics

Let us start from the equation for the electric field of a monochromatic electromagnetic wave beam in a stationary spatially non-dispersive medium, namely,

$$\nabla \times \big(\nabla \times E(\kappa,x)\big) - \kappa^2 \varepsilon(\kappa,x) E(\kappa,x) = 0, \qquad (1)$$

which is written in the dimensionless form adopted by Pereverzev[9], where the coordinates $x = (x^i)$, $i = 1,2,3$, are normalized to the scale L of typical spatial variations of the medium, and the large parameter

$$\kappa = \omega L/c,$$

is naturally singled out. (In addition, $\nabla = (\partial/\partial x^i)$ and c is the speed of light in free space.) The dependence of the solution $E(\kappa,x)$ on the parameter κ is explicitly indicated, whereas the additional dependence on the beam frequency ω in implied in both the electric field E and the dielectric tensor ε of the medium.

We are interested in asymptotic solutions of (1) in the limit $\kappa \to +\infty$, which, usually, can be constructed by modest computational means, and yet provide excellent approximations of the exact wave field for many applications where the parameter κ is very large; this constitutes an effective alternative to the major computational problem of direct numerical integration of (1) for very high frequencies in large three-dimensional domains.

As usual[6,9], the dielectric tensor is assumed to (be smooth and) have the asymptotic expansion,

$$\varepsilon(\kappa,x) = \varepsilon_0(x) + \kappa^{-1}\varepsilon_1(x) + O(\kappa^{-2}), \qquad (2)$$

in the limit $\kappa \to +\infty$, with ε_0 being Hermitian, i.e., $\varepsilon_0 = \varepsilon_0^*$; this implies that the medium is weakly dissipative, since the wave energy absorption coefficient[33] is related to the anti-Hermitian part $\varepsilon^a = \kappa^{-1}\varepsilon_1^a + O(\kappa^{-2})$, which is vanishingly small as $\kappa \to +\infty$. (Here, and throughout the paper $A^h = (A + A^*)/2$ and $A^a = -i(A - A^*)/2$ denote the Hermitian and anti-Hermitian part of a matrix A, respectively, and A^* denotes the Hermitian conjugation, i.e., the transpose of the complex-conjugate of A.)

Upon testing the wave operator, i.e., the left-hand side of equation (1), with a plane wave $e^{i\kappa N\cdot x}$, where $N = (N_i)$, $i = 1,\ldots,3$, is the refractive index vector, and separating the leading order in κ, one obtains the matrix-valued smooth function

$$D_{0,ij}(x,N) = N^2\delta_{ij} - N_iN_j - \varepsilon_{0,ij}(x), \qquad (3)$$

which is known as the dispersion tensor of the considered medium[6,34], or, mathematically, the semiclassical principal symbol[6,35] of the operator (1). This is defined on a

domain in the x-N space, which is referred to as the wave phase space.

The (real) eigenvalues of D_0 give the local dispersion functions of wave modes supported by the medium[6,36]; it is customary to assume that such eigenvalues, λ_j, are well separated, namely, there exists a strictly positive constant $C > 0$ such that $|\lambda_i(x,N) - \lambda_j(x,N)| \geq C$ for $i \neq j$ and for (x,N) in the relevant domain in the wave phase-space[7]; this implies that the dispersion surface of one mode does not get close to that of the other modes, i.e., linear mode conversion is excluded[6,7]: no energy exchange can take place among different modes, which can be singly studied. Let us denote by $H(x,N)$ the eigenvalue of $D_0(x,N)$ relevant to the considered mode, and let $e(x,N)$ be the corresponding unit eigenvector (for simplicity, we consider the case of simple eigenvalues, i.e., the corresponding eigenspace is assumed to be one-dimensional; the general case can be dealt with by using spectral projectors[7,37]).

The geometrical optics solution of equation (1) is constructed on the basis of a bundle of rays, which are defined as the spatial projections $x(\tau)$ of zero-energy phase-space orbits $\big(x(\tau), N(\tau)\big)$ of the Hamiltonian system,

$$\frac{dx^i}{d\tau} = \frac{\partial H}{\partial N_i}, \quad \frac{dN_i}{d\tau} = -\frac{\partial H}{\partial x^i}, \tag{4}$$

subject to the local dispersion relation (zero energy condition), $H\big(x(\tau), N(\tau)\big) = 0$.

Geometrical optics rays are the characteristics of the Hamilton-Jacobi equation[38] (also known as eikonal equation in this context),

$$H\big(x, \nabla S(x)\big) = 0, \tag{5a}$$

for the (real) eikonal function $S(x)$, which gives the phase of the wave field, while the amplitude transport equation

$$V(x)\cdot\nabla A(x) = \big[-\gamma_1(x) + i\delta_1(x) - \tfrac{1}{2}\nabla\cdot V(x)\big]A(x), \tag{5b}$$

determines the complex amplitude $A(x)$ of the wave field. Here, $V(x) = \partial H\big(x, \nabla S(x)\big)/\partial N$ plays the role of the group velocity,

$$\gamma_1 = e^* \cdot \varepsilon_1^a e, \tag{6}$$

accounts for wave damping, and

$$\delta_1 = e^* \cdot \varepsilon_1^h e + i e^* \cdot \{H, e\} - \frac{i}{2}\sum_{i,j} D_{0,ij}\{e_i^*, e_j\}, \tag{7}$$

accounts for a lower order shift in the phase, due to the residual Hermitian part ε_1^h (usually zero) plus the effects of polarization transport extensively discussed by Littlejohn and Flynn[36] and by Emmrich and Weinstein[37]; here, e_i are the components of e, and it is more convenient to define Poisson brackets by[39,40]

$$\{f, g\} = \frac{\partial f}{\partial N_i}\frac{\partial g}{\partial x^i} - \frac{\partial f}{\partial x^i}\frac{\partial g}{\partial N_i},$$

with the reversed order with respect to, e.g., Littlejohn and Flynn[36]. (The usual convention for the sum over repeated up- and down-placed indices is adopted throughout the paper.) In both equations (6) and (7), the right-hand side should be evaluated at $N = \nabla S(x)$; furthermore, the operator $V\cdot\nabla$ amounts to the derivative in the direction of geometrical optics rays, along which the amplitude is transported, and $\nabla\cdot V$ accounts for the effect of focusing/defocusing of rays.

The main result of geometrical optics can now be stated: given a (sufficiently regular) *classical* solution $S(x)$ and $A(x)$ of equations (5) in a bounded domain, and setting $a_0(x) = A(x)e\big(x, \nabla S(x)\big)$, there exists a corrector $a_1(x)$, such that the geometrical optics solution,

$$E_{\mathrm{GO}}(\kappa, x) = e^{i\kappa S(x)}\big(a_0(x) + \kappa^{-1}a_1(x)\big), \tag{8}$$

solves (1) with a remainder

$$|\kappa^{-2}\mathcal{L}(\kappa, x, \nabla)E_{\mathrm{GO}}(\kappa, x)| \leq C\kappa^{-2}, \tag{9}$$

uniformly for x in the considered domain; here, $\mathcal{L}(\kappa, x, \nabla)$ is the operator on the left-hand side of equation (1), and $C > 0$ is a constant. (The leading order term in (1) is $O(\kappa^2)$, hence, the whole equation has been multiplied by κ^{-2}.) The error estimate (9) just controls the reminder in the wave equation, but it does not say anything about the convergence of the geometrical optics solution to the exact solution; that would require a finer analysis[7].

In practice, the correction $a_1(x)$ is never evaluated, and yet it is important to take it into account, as the transport equation (5b) for the amplitude of the leading order term is obtained from the solvability condition for the linear algebraic problem that determines $a_1(x)$.

It is worth noting that both the phase $S(x)$ and the complex amplitude $A(x)$ can be obtained by a straightforward integration along each ray (ray tracing), with great advantages on the computational side. The phase $S(x)$, in particular, is obtained by integrating $dS = N\cdot dx$ along rays, cf. equation (5a).

In addition to its computational advantages, the foregoing asymptotic result allows us to extract a relevant physical information: the wave energy density is transported along geometrical optics rays. More specifically, equation (5b) can be recast in the form[5] (after some algebra and restoring dimensional quantities)

$$\nabla_r \cdot \big[v_g W\big] = -\gamma W, \tag{10}$$

where ∇_r denotes the gradient in physical (dimensional) coordinates,

$$v_g = -\frac{\partial H/\partial k}{\partial H/\partial\omega} = c\left|\frac{\partial(\omega H)}{\partial\omega}\right|^{-1}\frac{\partial H}{\partial N}, \tag{11}$$

is the group velocity[33],

$$W = \left|\frac{\partial(\omega H)}{\partial\omega}\right|\frac{|A|^2}{16\pi} = \frac{1}{\omega}\left[e^*\cdot\frac{\partial(\omega^2\varepsilon_0)}{\partial\omega}e\right]\frac{|A^2|}{16\pi}, \tag{12}$$

is the total wave energy density, comprising the electric, magnetic, and sloshing energy[33,34], and

$$\gamma = \left|\frac{\partial(\omega H)}{\partial\omega}\right|^{-1} 2\gamma_1, \tag{13}$$

is the energy absorption coefficient. Here, all derivatives with respect to the frequency are taken at constant wave vector $k = \omega N/c$, and phase-space functions are evaluated at $N = \nabla S$.

The aim of this paper is the precise derivation of an energy conservation law analogous to (10) in the framework of complex geometrical optics.

B. Caustics and the emergence of complex phases

Before presenting the main results of this work, let us briefly recall the basic arguments for the introduction of a complex eikonal function: we shall see that a complex eikonal emerges naturally from geometric asymptotics[40–43] of the wave field near points where a classical solution of the eikonal equation (5a) is not available, i.e., near caustics. We follow here the argument of De Micheli and Viano[44], which is based on the Ludwig system of partial differential equations[45].

Let us start noting that the error estimate (9) relies on the existence of a *classical* solution of the Hamilton-Jacobi equation (5a) (when that exists, the transport equation (5b) is automatically well posed).

A problem arises when a classical solution of (5a) is not available in the considered domain. Roughly speaking, this happens when geometrical optics rays cross each other: each ray carries a different value of the phase $S(x)$, which, then, becomes multi-valued at points where rays cross each other. Near a generic point x of the domain, such multiple values can, typically, be singled out into a finite number of phase functions $S_i(x)$, that can be thought of as different branches of the considered wave mode. To each branch, one can associate a velocity field $V_i(x) = \partial H\big((x, \nabla S_i(x)\big)/\partial N$, as well as coefficients $\gamma_{1,i}(x)$ and $\delta_{1,i}(x)$, defined by equations (6) and (7) evaluated at $N = \nabla S_i(x)$, and construct a *local* approximation of the wave field as a sum of the geometrical optics solutions of the form (8), one for each branch. Unfortunately, however, such a construction has no hope to give a *uniform* approximation of the wave field, as there are, in general, particular points where $\nabla\cdot V_i$ has a singularity, which makes the amplitude $A_i(x)$ blow-up. Such points are known as caustics, for, there, the exact solution exhibits a large (but finite) peak of intensity[46–48].

From a physical point of view, the validity of geometrical optics has been investigated by Kravtsov and Orlov[5,49], with the result that, roughly speaking, near caustics the geometrical optics solution (8) fails to account for wave effects, such as diffraction[4].

Caustics are extremely common and their occurrence is not related to the complexity of the medium: even in very simple media, e.g., uniform and isotropic, caustics can easily be generated depending on boundary conditions.

Let us assume, as boundary conditions, that the wave field is prescribed in the form $E_0(\kappa, y) \propto e^{i\kappa S_0(y)}$ on a $(d-1)$-dimensional smooth surface

$$\Sigma_0 = \{x;\ x = x_0(y)\},$$

parametrized by the variables $y = (y^i)$, $i = 1, \dots, d-1$, where $d \geq 2$ is the effective dimensionality of the problem (typically, $d = 2$ or $d = 3$); one can think of Σ_0 as the surface of either a mirror or an antenna, where the launched wave field is known.

The gradient of the initial phase $S_0(y)$, together with the local dispersion relation $H\big(x_0(y), N_0(y)\big) = 0$, yields the initial conditions $\big(x_0(y), N_0(y)\big)$ for Hamilton's equations (4); physically meaningful data must be such that the lifted surface

$$\Lambda_0 = \{(x, N);\ x = x_0(y),\ N = N_0(y)\}, \tag{14}$$

is non-characteristic[38], i.e., the Hamiltonian orbits of the system (4) originating from points of Λ_0 are transversal to Λ_0 itself (orbits must move away from the surface). Then, the solution of Hamilton's equations (4) can be readily found in the form $\big(x(\tau, y), N(\tau, y)\big)$ depending on the initial point y on the launching surface Σ_0. This defines a d-dimensional surface

$$\Lambda = \{(x, N);\ x = x(\tau, y),\ N = N(\tau, y)\}, \tag{15}$$

immersed into the $2d$-dimensional wave phase space, and parametrized by coordinates (τ, y); indeed, Λ is the flow out of Λ_0 by the Hamiltonian flow. (One could check that Λ_0 is an isotropic manifold, and, thus, Λ is a Lagrangian manifold[40–43], but these properties will not be explicitly needed in the following simplified presentation.)

The calculation of the integral of $dS = N \cdot dx$ along rays gives the phase $S(\tau, y)$. In order to complete the construction of the eikonal function $S(x)$ satisfying (5a), the standard method of characteristics[38] requires that the mapping $(\tau, y) \mapsto x = x(\tau, y)$ is inverted, i.e., (τ, y) needs to be written as a function of x. Physically, given the observation point x, we are asking for which initial point y a ray reaches the position x. Geometrically, that is equivalent to saying that the projection $(x, N) \mapsto x$, from the wave phase space onto the configuration space, defines a one-to-one relationship between Λ and the configuration space. When that is the case, Λ is the graph of $\nabla S(x)$, and $S(x)$ is the desired solution of (5a).

Figure 1 shows the surface Λ for three models in two dimensions ($d = 2$). In those cases, the phase space is four-dimensional, and yet one can obtain an effective visualization of Λ by exploiting the local dispersion relation to eliminate one dimension; this visualization concept has been recently suggested by Tracy et al.[50]. Here, the simple case of transverse electromagnetic waves in an isotropic medium has been considered, for which the local dispersion relation reads[5]

$$H(x, N) = N^2 - n^2(x) = 0, \tag{16}$$

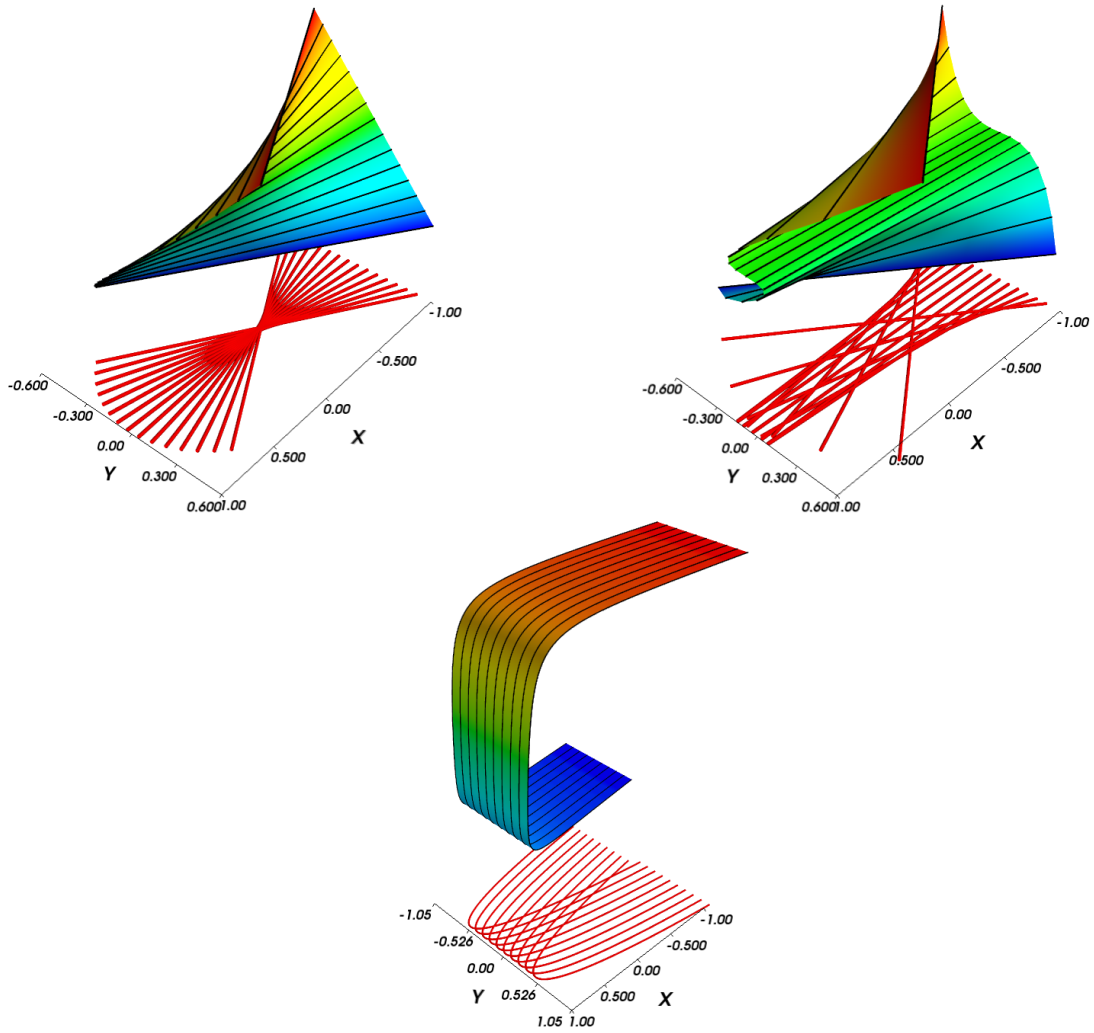

FIG. 1. Visualization of Lagrangian surfaces in two dimensions for three models of wave propagation corresponding to the local dispersion relation (16): parabolic focal point in free space (upper-left panel), quartic focal point in free-space (upper-right panel), and a fold caustic (lower panel). The curves in the x-y plane represent selected rays, while the curves on the Lagrangian surface represent the corresponding Hamiltonian orbits in the phase space.

$n(x)$ being the refractive index. In two dimensions, let us write $x = (x^1, x^2) = (\mathsf{x}, \mathsf{y})$ and $N = (N_1, N_2) = (N_\mathsf{x}, N_\mathsf{y})$. Then, the dispersion manifold can be parametrized by $(\mathsf{x}, \mathsf{y}, \alpha)$, with $N_\mathsf{x} = n(\mathsf{x}, \mathsf{y}) \cos\alpha$, $N_\mathsf{y} = n(\mathsf{x}, \mathsf{y}) \sin\alpha$, and the angle α is used as a third axis in figure 1; the initial surface is $\Sigma_0 = \{(\mathsf{x}, \mathsf{y});\ \mathsf{x} = -1\}$, and the beam is launched toward the positive x-axis. The case of free space, $n(\mathsf{x}, \mathsf{y}) = 1$, is shown in the upper panels, for two different boundary conditions: parabolic launching mirror, $\alpha_{|\Sigma_0} \propto \mathsf{y}$, (upper-left panel) and a quartic launching mirror, $\alpha_{|\Sigma_0} \propto \mathsf{y}^3$, (upper-right panel); in the latter case the Lagrangian surface Λ exhibits a rather complicated structure despite the simplicity of the medium. The lower panel shows the classical case of reflection from a linear medium, for which, $n^2(\mathsf{x}, \mathsf{y}) = (1 - \mathsf{x})/2$, with a cut-off at $\mathsf{x} = 1$, where the refractive index vanishes; in this case, a plane wave is launched with angle $\alpha_{|\Sigma_0} = 8°$.

It is clear that, in all cases of figure 1, the surface Λ cannot be projected one-to-one on the configuration space. Particularly, one can note that there are points $x = (\mathsf{x}, \mathsf{y})$, above which Λ can be separated into a finite number branches, each one being horizontal, and, thus, representable as the graph $N = \nabla S_i$; these are the regular points. Such branches, however, merge in points where Λ turns vertical; those are the singular points of Λ, and their projection onto the configuration space defines the set of caustics.

Caustics pose an obstruction to the existence of classical solutions of the Hamilton-Jacobi equation for the phase, and, in the same way, they are at the basis of the amplitude blow-up, and of the consequent loss of uniform approximation. In order to see this, let us consider the Jacobian matrix $U(\tau, y)$ of the map $(\tau, y) \mapsto x(\tau, y)$. Since $x(\tau, y)$ solves an ordinary differential equation, one

can check that, in components,

$$\partial U^i_j/\partial\tau = (\nabla V)^i_k U^k_j,$$

and, for the determinant $|U| = \det U$,

$$\partial|U|/\partial\tau = \big(\nabla\cdot V\big)|U|;$$

these are well known properties of ordinary differential equations, cf. the first chapter of Hörmander's lectures[51]. Since $V\cdot\nabla = \partial/\partial\tau$, equation (5b) can be written as[5]

$$\begin{cases} A = |U|^{-\frac{1}{2}}\tilde{A}, \\ \partial\tilde{A}/\partial\tau = \big[-\gamma_1 + i\delta_1\big]\tilde{A}, \end{cases} \tag{17}$$

and the coefficients of the equation for $\tilde{A}$ are smooth on the whole wave phase space. Therefore, equation (17) for $\tilde{A}(\tau, y)$ can always be solved by a simple integration along the rays, and the results accounts for the amplitude damping and phase shift. The total amplitude A, on the other hand, depends on the Jacobian determinant $|U|$, which accounts for the convergence/divergence of the bundle of rays, or, in other words, for the deformation of the volume element along a ray tube. The determinant $|U|$ vanishes near singular points of Λ, thus, causing the blow-up of the amplitude near caustics. (For a rigorous coordinate-free argument, the reader can refer to Duistermaat[40,41], Hörmander[42] and Guillemin and Sternberg[43].)

It is erroneously believed that this obstruction could be overcome by adding higher order corrections to the geometrical optics solution (8). Let us observe, however, that the singularity is found already in the leading order term, i.e., the eikonal equation. In order to overcome this limitations, generalized solutions of the eikonal equation must be considered. A overview of methods, oriented toward computational aspects, can be found in the review paper by Runborg[52]. Methods for the direct numerical solution of the eikonal equation, including generalized solutions, on a fixed grid (Eulerian geometrical optics) are reviewed by Benamou[53]. Here, instead, we shall focus on the geometry of the bundle of rays (Lagrangian geometrical optics), or, more precisely, on the geometry of the manifold Λ.

One of the most powerful ideas is to consider the Lagrangian surface Λ itself as a generalized solution of the eikonal equation, and find the way to associate it to a wave field, which is then called Lagrangian distribution, and which gives the desired uniform approximation of the exact wave field. This idea goes back to Maslov[54], Hörmander and Duistermaat[40,42], cf. also Guillemin and Sternberg[43]; Lagrangian distributions for multi-component fields are discussed by Hansen and Röhrig[55]. Here, we give a simplified presentation, which eventually leads to the introduction of a complex eikonal function.

The key point is that the Lagrangian surface Λ can be represented in terms of a phase function $\varphi(x,\theta)$ depending on a number of auxiliary variables $\theta = (\theta^1, \dots, \theta^m)$. The phase is chosen so that the set of its stationary points,

$$C_\varphi = \{(x,\theta);\ \nabla_\theta\varphi(x,\theta) = 0\}, \tag{18}$$

immersed into the wave phase space by the mapping $(x,\theta)\mapsto(x,N)$, with

$$N = \nabla_x\varphi(x,\theta), \tag{19}$$

yields the Lagrangian surface Λ. It is a general result of symplectic geometry that such a phase can always be found, at least locally, and it is called a local parametrization of the Lagrangian surface[39,40,43].

Given such a parametrization, one can write the wave field as a superposition of a continuous family of eikonal waves with phase $\varphi(x,\theta)$ and amplitude $a(\kappa,x,\theta)\sim a_0(x,\theta) + \kappa^{-1}a_1(x,\theta) + \cdots$, cf. equation (8); that gives a uniform approximation of the wave field in the form

$$E(\kappa,x) = \Big(\frac{\kappa}{2\pi}\Big)^{\frac{m}{2}}\int e^{i\kappa\varphi(x,\theta)}a(\kappa,x,\theta)d\theta. \tag{20}$$

Since the integral in θ and the operator $\mathcal{L}(\kappa,x,\nabla)$ on the left-hand side of equation (1) commute, one finds $a_0(x,\theta) = A(x,\theta)e\big(x,\nabla_x\varphi(x,\theta)\big)$, as in the standard geometrical optics, $A(x,\theta)$ being a solution of (5b) with the coefficients in the definitions of V, γ, and δ evaluated at $N = \nabla_x\varphi(x,\theta)$.

Let us note that, since (20) is a superposition of eikonal waves, the result accounts for diffraction, in the same way as a superposition of plane waves does in a homogeneous medium. In addition, where the stationary phase set C_φ is horizontal over the configuration space, i.e., where the condition $\nabla_\theta\varphi(x,\theta) = 0$ defines a finite number of branches $\theta = \theta_i(x)$, the stationary phase lemma[40,56] can be applied to reduce the integral (20) to a finite sum of eikonal waves with phases $S_i(x) = \varphi\big(x,\theta_i(x)\big)$, one for each branch of Λ, as expected. The normalization $(\kappa/2\pi)^{m/2}$ in front of the integral in (20) is chosen to remove the analogous factor in the stationary phase lemma.

Simplified examples of such diffractive approximations of wave fields relevant to plasma waves can be found in the work of Richardson et al.[57] and Cairns and Fuchs[58], for the specific case of lower-hybrid beams, for which the description of caustics is particularly relevant.

Numerical methods for the general implementation of such an abstract construction in realistic applications are not yet available. Nevertheless, it is worth considering it in details, for one can draw deep insights on diffraction near caustics. Let us specialize it to an analytically tractable case.

We consider the simple, and yet physically relevant, model Hamiltonian (16), in presence of a fold caustic, like the one shown in figure 1, lower panel; this is typically used as a model of a beam reflected from a cut-off[59]. We try a parametrization with a single ($m = 1$) auxiliary variable θ, and a phase of the form (the specific form of φ depends on the considered caustic geometry[40])

$$\varphi(x,\theta) = u(x) + v(x)\theta - \tfrac{1}{3}\theta^3, \tag{21}$$

where the cubic term is chosen so that the stationary phase condition (18) is quadratic and accounts, at least locally, for the fold of Λ; specifically, the stationary phase set C_φ is determined by

$$v(x) - \theta^2 = 0. \tag{22}$$

For $v > 0$ (the illuminated region), C_φ has two branches, and the integral (20) can be evaluated by the stationary phase formula, yielding the sum for two eikonal wave fields, one for the incoming wave, which impinges on the cut-off, and one for the outgoing wave, which is reflected from the cut-off. At the zero-level set $v(x) = 0$ (the caustic set), the two branches merge and the stationary phase formula breaks down, so that the whole integral (20) should be considered. For $v(x) < 0$ (the shadow region), no stationary phase point exists, and the stationary phase lemma implies that the wave field (20) is exponentially small in the limit $\kappa \to +\infty$.

For (x, θ) satisfying (22), we need $N = \nabla_x \varphi(x, \theta)$ to fulfill the local dispersion relation (16), in order to reproduce the surface Λ. That yields a differential equation for $u(x)$ and $v(x)$, namely,

$$(\nabla u)^2 + (\nabla v)^2\theta^2 + 2(\nabla u \cdot \nabla v)\theta - n^2 = 0, \quad v = \theta^2.$$

In the shadow region, $v < 0$ and θ is purely imaginary, hence, the equation splits into

$$\begin{cases} (\nabla u)^2 + v(\nabla v)^2 - n^2 = 0, \\ \nabla u \cdot \nabla v = 0. \end{cases} \tag{23}$$

This is the *Ludwig eikonal system* of first-order partial differential equations[45], which can be viewed as a deformation of the eikonal equation $(\nabla u)^2 - n^2(x) = 0$ for an isotropic medium[5], controlled by the additional function v, with the gradient ∇v being tangent to phase fronts $u =$ constant. Equipped with appropriate boundary conditions, equations (23) yield a parametrization of Λ near a fold caustic. Upon introducing the complex phase,

$$\psi(x) = u(x) + i\tfrac{2}{3}(-v)^{\frac{3}{2}}, \tag{24}$$

the Ludwig system (23) is equivalent to the complex eikonal equation for an isotropic medium[16–20]

$$(\nabla \psi)^2 - n^2(x) = 0, \tag{25}$$

and this is obtained here only on the basis of the geometry of the Lagrangian surface Λ, which, in turn, is obtained by standard ray tracing.

One can also observe that, in the illuminated region $v > 0$, the phase has two real-valued branches, namely,

$$\psi_\pm(x) = u(x) \pm \tfrac{2}{3}v^{3/2}(x), \quad (v(x) > 0), \tag{26}$$

while, in the shadow region $v < 0$, one has

$$\psi(x) = u(x) + i\tfrac{2}{3}|v(x)|^{3/2}, \quad (v(x) < 0), \tag{27}$$

where the second branch of the square root is ignored by imposing the physical condition that the field should be bounded for $\kappa \to +\infty$.

At last, let us consider the lowest order term in the wave field (20). With the change of variable $\theta = -\kappa^{-1/3}\xi$, and for any non-negative integer n, one has

$$\int \theta^n e^{i\kappa(v\theta - \theta^3/2)} d\theta = 2\pi i^n \kappa^{-(n+1)/3} \mathrm{Ai}^{(n)}(-\kappa^{2/3}v),$$

where $\mathrm{Ai}^{(n)}(z) = d^n\mathrm{Ai}(z)/dz^n$ is the n-th order derivative of the Airy function,

$$\mathrm{Ai}(z) = \frac{1}{2\pi}\int e^{i(\xi^3/3 + z\xi)} d\xi.$$

With reference to the Taylor expansion of the amplitude,

$$a_0(x, \theta) = g_0(x) + \theta g_1(x) + \cdots,$$

the term $\sim \theta^n$ gives a contribution of order $\kappa^{-(n+1)/3}$. Consistently with neglecting terms of order κ^{-1}, we need to keep the first two terms only, and, thus,

$$\begin{aligned} E(\kappa,x) = \sqrt{2\pi\kappa} e^{i\kappa u(x)} \Big[& g_0(x)\mathrm{Ai}\big(-\kappa^{2/3}v(x)\big)/\kappa^{1/3} \\ & + i g_1(x)\mathrm{Ai}'\big(-\kappa^{2/3}v(x)\big)/\kappa^{2/3} + O(\kappa^{-1})\Big]. \end{aligned} \tag{28}$$

Let us recall once more that the occurrence of the Airy function is a consequence of the specific geometry of a fold, which guided the selection of the phase (21). Other types of caustics will have a different parametrization leading to a different field profile; a classification of caustics and their generating phases is a major result of catastrophe theory[40,46].

As an example, let us go back to the two-dimensional model of figure 1, lower panel, which corresponds to a plane wave launched into a linear medium, with the refractive index $n^2(\mathsf{x}) = (1 - \mathsf{x})/2$, independent of y; then, one of the two spatial variables, namely, y, is ignorable. We can try to obtain a solution of (23) by setting $u(\mathsf{x}, \mathsf{y}) = N_\mathsf{y}\mathsf{y}$, N_y being the constant y-component of the refractive index vector, and taking $v(\mathsf{x}, \mathsf{y}) = v(\mathsf{x})$, independent of y. The Ludwig system reduces to an ordinary differential equation for $v(\mathsf{x})$, namely,

$$v(v')^2 = n^2(\mathsf{x}) - N_\mathsf{y}^2,$$

with $v' = dv/d\mathsf{x}$; this is readily solved, yielding

$$v(\mathsf{x}) = 2^{-1/3}(1 - \mathsf{x} - 2N_\mathsf{y}^2). \tag{29}$$

It remains to compute the amplitudes $g_j(x)$, $j = 0, 1$. For the specific case of a transverse wave with constant polarization in an isotropic medium with $\varepsilon_1 = 0$, the relevant equation for the lowest order amplitude is $\nabla_x\varphi(x, \theta) \cdot \nabla_x A(x, \theta) = 0$, which admits constant solutions. Particularly, no singularity is found, in contrast to the standard formulation based on classical solutions for the eikonal S.

The function g_0 can then be regarded as constant and $g_1 = 0$, so that, accounting for (29), the wave field amounts to

$$E(\kappa, \mathsf{x},\mathsf{y}) = \sqrt{2\pi}\kappa^{1/6} g_0 e^{i\kappa N_\mathsf{y}\mathsf{y}} \times \mathrm{Ai}\big(2^{-\frac{1}{3}}\kappa^{\frac{2}{3}}(\mathsf{x} + 2N_\mathsf{y}^2 - 1)\big) + O(\kappa^{-1/2}). \tag{30}$$

One can check that the electric field (30) solves exactly equation (1), which, for the example under consideration, reduces to the Helmholtz equation[59],

$$\Delta E + \kappa^2 n^2 E = 0, \quad n^2(\mathsf{x}) = \tfrac{1}{2}(1 - \mathsf{x}),$$

with boundary conditions given at $\mathsf{x} = -1$ and representing a plane wave with refractive index N_y. (Here, Δ is the Laplace operator in the (x, y)-plane.)

It is remarkable that an exact diffractive solution can be obtained using only geometrical optics rays, provided that the geometry of the corresponding Lagrangian surface is properly accounted for. This proves that geometrical optics rays do carry information on diffraction.

Nonetheless, the procedure described in this section is extremely complex and a direct numerical implementation in complicated three-dimensional geometries does not appear viable yet.

On the other hand, the method itself shows that a complex-valued phase, cf. equation (24), encodes all the information on the caustic geometry. In particular, the complex eikonal equation (25) is equivalent to the Ludwig system (23). It is worth noting also that, near a caustic, fractional powers of the the small parameter κ^{-1} appear in the asymptotics of the wave field[4], as opposed to the conventional asymptotic expansion (8) in integer powers of κ^{-1}.

In the next section, the general theory of complex geometrical optics is developed, with particular care for the energy transport. Fractional powers of κ^{-1} will play an important role in the derivation of the energy transport equation.

III. GENERAL THEORY OF COMPLEX EIKONAL

For practical applications, the construction of Lagrangian distributions outlined in section II B is not yet viable, as appropriate numerical methods do not appear to be mature. Nevertheless, Lagrangian distributions suggest that the introduction of a complex phase might help avoiding some type of caustic singularities.

For instance, in the solution (28) of the cut-off reflection problem, the asymptotic expansion of the Airy function for $\kappa \to +\infty$ and $v(x) \neq 0$ yields

$$E(\kappa, x) = \frac{g_0}{\sqrt{2}|v|^{1/4}} \times \begin{cases} e^{-i\frac{\pi}{4}}\big[e^{i\kappa\psi_+} + e^{i\kappa\psi_- + i\frac{\pi}{2}}\big], & v(x) > 0, \\ e^{i\kappa\psi}, & v(x) < 0, \end{cases}$$

where the complex phases $\psi_\pm$ and ψ are defined in (26) and (27), respectively.

This has a clear physical interpretation: in the illuminated region ($v > 0$), the solution is composed of two waves, one propagating toward the cut-off with phase ψ_+ and the other one being reflected from the cut-off with phase ψ_- and a shift of $\pi/2$, due to the reflection. In the evanescent region ($v < 0$), one has an exponentially small shadow field with phase ψ. All three branches of the wave field can be represented by a complex phase, which, in particular, attains purely real values in the illuminated region.

The foregoing asymptotic expansion still blows up on the caustic $v = 0$, where $E(\kappa, x) \sim |v|^{-1/4}$. However, this suggests that an asymptotic solution of the form (8), where the phase S is replaced by a complex valued function ψ, might capture both propagating and evanescent fields, and, thus, diffraction effects. Such an approach will not be as general as geometric asymptotics of section II B, and it can still be prone to caustic singularities (as shown in the foregoing asymptotic expansion). On the other hand, it can successfully deal with a class on important diffractive solutions, namely, focused and collimated beams.

A. Paraxial character of complex eikonal waves

Guided by the foregoing argument, let us search for asymptotic solutions of equation (1) in the form of a complex eikonal wave, namely,

$$E_{\mathrm{CGO}}(\kappa, x) = e^{i\kappa\psi(x)} a(\kappa, x), \tag{31a}$$

where $\psi(x) = S(x) + i\phi(x)$, $\phi(x) \geq 0$, is the complex eikonal,

$$a(\kappa, x) \sim a_0(x) + \kappa^{-1} a_1(x) + \cdots, \tag{31b}$$

and the amplitudes $a_k(x)$ are independent of κ and bounded in x; then, the asymptotic sum $a(\kappa, x)$ is also bounded[35], and we write,

$$|a(\kappa, x)| \leq C_0, \quad \text{for } \kappa \geq \kappa_0,$$

where $C_0 > 0$ and $\kappa_0 > 1$ are constants. The condition $\phi(x) \geq 0$ on the imaginary part of the eikonal is required by the boundedness of the wave field for $\kappa \to +\infty$.

Ansatz (31) should now be substituted into the wave equation (1). Before proceeding, however, let us make two important observations, first noted by Pereverzev[9] and Maslov[10] independently. Both are consequences of the condition $\phi(x) \geq 0$ and imply that the wave field (31a) is *paraxial*.

The first observation is that the wave field (31a) is exponentially small, in the limit $\kappa \to +\infty$ near points x where $\phi(x) > 0$; indeed, one has $|E(\kappa, x)| \propto e^{-\kappa\phi(x)} \to 0$ for $\kappa \to +\infty$, or, more precisely, for every integer $n > 0$,

$$\kappa^n |E_{\mathrm{CGO}}(\kappa, x)| \leq C_0 \Big(\frac{n}{e\phi(x)}\Big)^n, \quad \phi(x) > 0, \tag{32}$$

which is tantamount to exponential decay.

The second observation requires some preparation. Estimate (32) means that the wave field (31a), in the limit $\kappa \to +\infty$, collapses on the zero-level set of the function $\mathrm{Im}\psi = \phi$, namely,

$$\mathcal{R} = \{x;\ \phi(x) = 0\}. \tag{33}$$

For instance, in the case of a fold caustic studied in section II B, the set $\mathcal{R}$ encloses the whole illuminated region $v(x) > 0$ up to and including the caustic $v(x) = 0$, while the field is indeed exponentially small in the remaining shadow region $v(x) < 0$.

Let us restrict our attention to a much simpler case. Let the set $\mathcal{R}$ be a curve given parametrically by $x = \bar{x}(\tau)$. In the paraxial WKB theory, this is called reference ray[9].

By definition $\phi\big(\bar{x}(\tau)\big) = 0$, identically in τ and,

$$0 = \frac{d}{d\tau}\phi\big(\bar{x}(\tau)\big) = \frac{d\bar{x}(\tau)}{d\tau} \cdot \nabla\phi\big(\bar{x}(\tau)\big),$$

which means that the component of $\nabla\phi\big(\bar{x}(\tau)\big)$ tangent to the curve $\mathcal{R}$ vanishes identically; the other two components must vanish as well, otherwise ϕ would change sign across $\mathcal{R}$, thus, violating the condition $\phi \geq 0$. It follows that

$$\nabla\phi\big(\bar{x}(\tau)\big) = 0,$$

identically in τ. Then, the Taylor polynomial of ϕ around $\bar{x}$ has terms of second order or higher only. Continuing, one has

$$0 = \frac{d}{d\tau}\nabla\phi\big(\bar{x}(\tau)\big) = D^2\phi\big(\bar{x}(\tau)\big)\frac{d\bar{x}(\tau)}{d\tau},$$

where $D^2\phi(x) = \big(\partial^2\phi(x)/\partial x^i \partial x^j\big)$ is the Hessian matrix of second-order derivatives of ϕ. Thence, the tangent vector $e_t(\tau) \propto d\bar{x}(\tau)/d\tau$ is an eigenvector of $D^2\phi\big(\bar{x}(\tau)\big)$ corresponding to the null eigenvalue.

In general, the whole matrix $D^2\phi(\bar{x})$ can be zero, and, in that case, Taylor polynomial of ϕ would have only terms of fourth order or higher (the third order is again excluded by the condition $\phi \geq 0$). For definiteness, we shall consider the case in which, except for the tangent direction $\propto e_t$, the matrix $D^2\phi(\bar{x})$ is strictly positive definite. Precisely,

$$w \cdot D^2\phi\big(\bar{x}(\tau)\big)w > 0, \tag{34}$$

for every vector w linearly independent of $e_t(\tau)$, i.e., $D^2\phi$ is positive definite for vectors transversal to the reference curve $\mathcal{R}$.

The exact Taylor formula for ϕ now reads,

$$\phi(x) = \frac{1}{2}(x - \bar{x}) \cdot Q(x, \bar{x})(x - \bar{x}),$$

where, for $|x - \bar{x}|$ small enough, the matrix-valued function,

$$Q(x, \bar{x}) = 2\int_0^1 D^2\phi\big((1-s)\bar{x} + sx\big)(1-s)ds,$$

is positive definite for vectors transversal to the reference curve $\mathcal{R}$. Through diagonalization of the symmetric matrix Q, one can find $B(x, \bar{x})$ such that

$$Q(x, \bar{x}) = {}^tB(x, \bar{x})B(x, \bar{x}),$$

where ${}^tB$ denotes the transpose of B. With the new function $\xi(x) = B(x, \bar{x})(x - \bar{x})$, the imaginary part of the complex phase becomes

$$\phi(x) = \frac{1}{2}\xi^2(x).$$

This form of the imaginary part ϕ is valid in a neighborhood of $\mathcal{R}$ only and it is of dubious practical utility, except for obtaining the following inequality[9]

$$|\xi(x)^\alpha e^{-\kappa\phi(x)}| = |z^\alpha e^{-z^2/2}|\kappa^{-|\alpha|/2} \leq C_\alpha \kappa^{-|\alpha|/2},$$

where the multi-index notation has been used: the vector of integers $\alpha = (\alpha_1, \ldots, \alpha_d)$ is the multi-index, with length $|\alpha| = \alpha_1 + \cdots + \alpha_d$, and $\xi^\alpha = (\xi^1)^{\alpha_1} \cdots (\xi^d)^{\alpha_d}$. Here, $z = \sqrt{\kappa}\xi$ and $C_\alpha > 0$ is a constant depending only on α. Roughly speaking, every time one multiplies the exponential $e^{-\kappa\phi}$ by any component ξ^i, the order is reduced by a factor $1/\sqrt{\kappa}$. On noting that $\nabla\phi(x) = \delta_{ij}(\nabla\xi^i(x))\xi^j(x)$, one has

$$|(\nabla\phi)^\alpha e^{i\kappa\psi}| \leq C_\alpha \kappa^{-|\alpha|/2}, \tag{35}$$

where C_α is a different constant. This is the second consequence of the ansatz (31a).

Differently from estimate (32), however, (35) is not fully general as it relies on the assumptions that (i) the set (33) is a curve, and (ii) the matrix $D^2\phi$ satisfies (34). The latter condition, in particular, is the reason for which half-integer powers of $1/\kappa$ are found. We shall see that this is the appropriate setting for studying focused beams, for which the caustic geometry is similar to the one represented in figure 1, upper-left panel. This is the situation of practical interest for electromagnetic wave beams in fusion plasmas.

B. Complex eikonal theory

The substitution of the ansatz (31a) into Maxwell's wave equation (1) for the electric field yields

$$e^{i\kappa\psi}\Big\{\kappa^2 D_0(x, \nabla\psi)a_0(x) + \kappa\Big[D_0(x, \nabla\psi)a_1 - i\Big[\frac{\partial D_0}{\partial N_i}(x, \nabla\psi)\frac{\partial a_0}{\partial x^i} + \frac{1}{2}\frac{\partial}{\partial x^i}\Big[\frac{\partial D_0}{\partial N_i}(x, \nabla\psi)\Big]a_0 - i\varepsilon_1 a_0\Big]\Big]\Big\} + O(1) = 0, \tag{36}$$

where equation (2) has been accounted for. In writing equation (36), one should note that the dispersion tensor D_0, defined in equation (3) is a polynomial in N, and,

thus, it extends to an entire function of the complex refractive index $\tilde{N} = N + iN'$, which has been evaluated at $\tilde{N} = \nabla\psi$. The same argument applies to the derivatives of D_0; explicitly,

$$D_{0,ij}(x, \nabla\psi) = (\nabla\psi)^2\delta_{ij} - \frac{\partial\psi}{\partial x^i}\frac{\partial\psi}{\partial x^j} - \varepsilon_{0,ij}(x), \quad (37a)$$

$$\frac{\partial D_{0,ij}}{\partial N_k}(x, \nabla\psi) = 2\frac{\partial\psi}{\partial x^l}\delta^{lk}\delta_{ij} - \delta_i^k\frac{\partial\psi}{\partial x^j} - \frac{\partial\psi}{\partial x^i}\delta_j^k, \quad (37b)$$

$$\frac{\partial^2 D_{0,ij}}{\partial N_k \partial N_l}(x, \nabla\psi) = 2\delta^{kl}\delta_{ij} - \delta_i^k\delta_j^l - \delta_i^l\delta_j^k, \quad (37c)$$

while

$$\begin{aligned}&\frac{\partial}{\partial x^i}\Big[\frac{\partial D_0}{\partial N_i}(x, \nabla\psi)\Big] \\ &\quad = \frac{\partial^2 D_0}{\partial x^i \partial N_i}(x, \nabla\psi) + \frac{\partial^2\psi}{\partial x^i\partial x^j}\frac{\partial^2 D_0}{\partial N_i \partial N_j}(x, \nabla\psi).\end{aligned} \quad (38)$$

The first term on the right-hand side of (38) is actually zero for the dispersion tensor (3), and the second-order derivative with respect to N is constant, cf. equation (37c). In the following, we keep both terms formally general. This generalization will be needed for spatially dispersive media in section V.

When one neglects the paraxial character of the wave field discussed in section III A, terms of different order in κ are separated in (36), yielding a hierarchy of equations for ψ, a_0, and a_1. Such equations, although formally similar to the corresponding equations of standard geometrical optics[36], are complicated by the presence of the imaginary part of the phase. The hierarchy thus obtained, however, is unnecessarily too strong, and it can be considerably simplified by taking into account the paraxial character of complex eikonal waves, as quantified by inequalities (32) and (35).

Inequality (35), in particular, implies that a few terms in equation (36), precisely those proportional to $\mathrm{Im}\nabla\psi = \nabla\phi$, can be better estimated by half-integer powers of κ.

When that is accounted for, equation (36) becomes

$$\begin{aligned}&e^{i\kappa\psi}\Bigg\{\kappa^2 D_0(x, \nabla\psi)a_0(x) \\ &\quad + \kappa\Bigg[D_0(x, \nabla S)a_1 - i\Big[\frac{\partial D_0}{\partial N_i}(x, \nabla S)\frac{\partial a_0}{\partial x^i} \\ &\quad + \frac{1}{2}\Big[\frac{\partial^2 D_0}{\partial x^i \partial N_i}(x, \nabla S) + \frac{\partial^2\psi}{\partial x^i\partial x^j}\frac{\partial^2 D_0}{\partial N_i\partial N_j}(x, \nabla S)\Big]a_0 \\ &\quad - i\varepsilon_1 a_0\Big]\Big]\Bigg\} + O(\sqrt{\kappa}) = 0.\end{aligned} \quad (39)$$

Now the imaginary part of the complex phase enters the $O(\kappa)$-term through the Hessian matrix $\partial^2\psi/\partial x^i\partial x^j$ only, a simplification which will be crucial in deriving the wave energy flux.

In order to solve the wave equation within an $O(\sqrt{\kappa})$-remainder (corresponding to an error of $O(\kappa^{-3/2})$ as the leading terms in the wave equation are of $O(\kappa^2)$), we can now exploit the linear independence of monomials κ^n for $\kappa \geq \kappa_0$, cf. comments after equation (31b), and separate the coefficients of κ^2 and κ. Here, estimate (35) can be exploited once more: a remainder of appropriate order in $\nabla\phi$ can be allowed. Specifically,

$$D_0(x, \nabla\psi)a_0 = \rho_0(x, \nabla\phi), \quad (40a)$$

$$\begin{aligned}&D_0(x, \nabla S)a_1 - i\Bigg[\frac{\partial D_0}{\partial N_i}(x, \nabla S)\frac{\partial a_0}{\partial x^i} \\ &\quad + \frac{1}{2}\Big[\frac{\partial^2 D_0}{\partial x^i\partial N_i}(x, \nabla S) + \frac{\partial^2\psi}{\partial x^i\partial x^j}\frac{\partial^2 D_0}{\partial N_i\partial N_j}(x, \nabla S)\Big]a_0 \\ &\quad - i\varepsilon_1 a_0\Bigg] = \rho_1(x, \nabla\phi),\end{aligned} \quad (40b)$$

where the remainders ρ_0 and ρ_1 must be, at least, cubic and linear in $\nabla\phi$, respectively. Let us remark that this is not a perturbative argument in $\nabla\phi$: in general, the remainders are by no means small, except in a narrow strip around the zero-level set (33), where the beam is localized.

In solving equations (40), one notes that all terms on the left-hand side are polynomials in $\nabla\phi$, and, thus, the arbitrary remainders ρ_0 and ρ_1 can be chosen in order to cancel out exactly all terms of order equal to or higher than the third and the first order, respectively; then, the remaining terms must sum up to zero, thus providing the equations for ψ, a_0, and a_1. If we can find the solution of such equations for ψ, a_0, and a_1, then, the coefficient of κ^2 in the asymptotic form (39) of the wave equation can be substituted by the cubic remainder ρ_0, and, analogously, the coefficient of κ can be replaced by ρ_1. Equation (35), in conclusion, shows that the result is of $O(\sqrt{\kappa})$, which is the desired error.

Solution of equation (40a). The matrix $D_0(x, \nabla\psi)$ is no longer Hermitian, even though $D_0(x, N)$ is Hermitian for a real valued refractive index N. Nonetheless, $D_0(x, \nabla\psi)$ is much simpler than a generic complex matrix, as it is the analytical continuation of a Hermitian matrix.

For the specific case of the dispersion tensor (3), one can check, e.g., by means of (37), that the identity

$$D_0(x, \tilde{N}) = \tilde{D}_0(x, \tilde{N}),$$

holds true, with $\tilde{N} = N + iN'$ and

$$\begin{aligned}\tilde{D}_0(x, \tilde{N}) &= D_0(x, N) \\ &\quad + i\frac{\partial D_0(x, N)}{\partial N_k}N'_k - \frac{1}{2}\frac{\partial^2 D_0(x, N)}{\partial N_k \partial N_l}N'_k N'_l.\end{aligned}$$

This defines a convenient complex extension of $D_0(x, N)$ up to second-order terms in the imaginary part N'. Such an apparently cumbersome way of rewriting $D_0(x, \tilde{N})$ allows us to exploit the properties of the Hermitian matrix $D_0(x, N)$. Besides, the form $\tilde{D}_0(x, \tilde{N})$ is naturally encountered for the case of spatially dispersive media treated in section V.

Consistently, given an eigenvector $e_j(x,N)$ of the Hermitian matrix $D_0(x,N)$ corresponding to the eigenvalue $\lambda_j(x,N)$, we define the complex extension of e_j by an analogous expression,

$$\begin{aligned}\tilde{e}_j(x,\tilde{N}) &= e_j(x,N)\\ &+ i\frac{\partial e_j(x,N)}{\partial N_k}N'_k - \frac{1}{2}\frac{\partial^2 e_j(x,N)}{\partial N_k \partial N_l}N'_k N'_l,\end{aligned} \tag{41}$$

as well as the complex extension of its dual,

$$\begin{aligned}\tilde{f}_j(x,\tilde{N}) &= e^*_j(x,N)\\ &+ i\frac{\partial e^*_j(x,N)}{\partial N_k}N'_k - \frac{1}{2}\frac{\partial^2 e^*_j(x,N)}{\partial N_k \partial N_l}N'_k N'_l,\end{aligned} \tag{42}$$

and the complex extension of the corresponding eigenvalue,

$$\begin{aligned}\tilde{\lambda}_j(x,\tilde{N}) &= \lambda_j(x,N)\\ &+ i\frac{\partial \lambda_j(x,N)}{\partial N_k}N'_k - \frac{1}{2}\frac{\partial^2 \lambda_j(x,N)}{\partial N_k \partial N_l}N'_k N'_l,\end{aligned} \tag{43}$$

where, again, $\tilde{N} = N + iN'$. (A mathematically complete presentation of this argument can be found in an unpublished note[60].)

Upon taking into account the eigenvalue equation $D_0 e_j = \lambda_j e_j$, together with its derivatives with respect to N, one gets the identity

$$D_0(x,\tilde{N})\tilde{e}_j(x,\tilde{N}) - \tilde{\lambda}_j(x,\tilde{N})\tilde{e}_j(x,\tilde{N}) = O(|N'|^3), \tag{44}$$

which shows that $\tilde{e}_j(x,\tilde{N})$ is close to an eigenvector of $\tilde{D}_0(x,\tilde{N})$ corresponding to the eigenvalue $\tilde{\lambda}_j$, with a remainder which is cubic in N'.

Identity (44) shows that equation (40a) (with the arbitrary cubic remainder) is solved by a complex eikonal $\psi(x)$ and an amplitude $a_0(x)$ such that

$$\tilde{H}(x,\nabla\psi) = 0, \tag{45a}$$
$$a_0(x) = A(x)\tilde{e}(x,\nabla\psi), \tag{45b}$$

where $\tilde{H}(x,\tilde{N})$ is the complex extension of the specific eigenvalue $H(x,N)$ relevant to the considered wave mode, $\tilde{e}(x,\tilde{N})$ is the complex extension of the corresponding eigenvector, and $A(x)$ is an arbitrary complex scalar amplitude.

Given the wave mode, solution (45a) is, indeed, the only possible solution of (40a). In order to see that, let us recall that the eigenvectors of a Hermitian matrix are complete, i.e., they span the whole space. This is expressed by the identity

$$I = \sum_j e_j(x,N)e^*_j(x,N), \tag{46}$$

which holds true for every (x,N) in the wave phase space; here, I is the identity matrix. By taking into account (46) and its derivatives with respect to N, one can check that the completeness relation holds for complex extended quantities as well, but with a usual cubic remainder, namely,

$$I - \sum_j \tilde{e}_j(x,\tilde{N})\tilde{f}_j(x,\tilde{N}) = O(|N'|^3). \tag{47}$$

In the same way, one can extend the orthogonality of eigenvectors, namely, $e^*_i(x,N)\cdot e_j(x,N) = \delta_{ij}$, which reads

$$\tilde{f}_i \cdot \tilde{e}_j - \delta_{ij} = O(|N'|^3). \tag{48}$$

Then, a generic amplitude vector can be written in the form

$$\begin{aligned}a_0(x) &= \sum_j \tilde{e}_j(x,\nabla\psi)\big(\tilde{f}_j(x,\nabla\psi)\cdot a_0(x)\big) + O(|\nabla\phi|^3),\\ &= \sum_j A_j(x)\tilde{e}_j(x,\nabla\psi) + O(|\nabla\phi|^3),\end{aligned}$$

and equation (40a) amounts to

$$\sum_j \tilde{\lambda}_j(x,\nabla\psi)A_j(x)\tilde{e}_j(x,\nabla\psi) + O(|\nabla\phi|^3) = \rho_0(x,\nabla\phi).$$

One can now apply $\tilde{f}_i$ on the left and use the orthogonality (48), thus, splitting the vector equation (40a) into three scalar equations,

$$\tilde{\lambda}_i(x,\nabla\psi)A_i(x) + O(|\nabla\phi|^3) = \tilde{f}_i(x,\nabla\psi)\cdot\rho_0(x,\nabla\phi), \tag{49}$$

for $i = 1,2,3$. The amplitude A_i can be different from zero only if $\tilde{\lambda}_i(x,\nabla\psi) = 0$. On the other hand, only one out of the three eigenvalues can fulfill this condition for a given complex phase ψ, otherwise the hypothesis of separability of eigenvalues λ_j stated in section II A would be violated in points $\big(x,\nabla S(x)\big)$, $S = \mathrm{Re}\psi$, for $x = \bar{x}(\tau)$, i.e., on the reference curve (33). It follows that, given a specific wave mode corresponding to a specific eigenvalue H, equation (45a) gives the only solution for that mode.

From a computational point of view, equation (45a) reduces to a system of two coupled Hamilton-Jacobi equations, namely,

$$\begin{cases} H(x,\nabla S) - \dfrac{1}{2}\dfrac{\partial^2 H(x,\nabla S)}{\partial N_i \partial N_j}\dfrac{\partial\phi}{\partial x^i}\dfrac{\partial\phi}{\partial x^j} = 0,\\ \dfrac{\partial H(x,\nabla S)}{\partial N_i}\dfrac{\partial\phi}{\partial x^i} = 0,\end{cases} \tag{50}$$

for the real part S and the imaginary part ϕ of the complex phase. This system have been previously derived on the basis of a heuristic perturbative argument controlled by $|\nabla\phi|/|\nabla S|$, which is assumed to be small. Despite $\nabla\phi$ is indeed small in the region of interest, i.e., in a neighborhood of the curve $\mathcal{R}$ where the beam is localized, cf. equation (33), from a mathematical point of view, such a procedure is totally unsound as, in equation (50), the second order term is balanced against the leading order

term, and this is not compatible with a precise perturbation argument. Our analysis resolves this inconsistency, recovering system (50) in a mathematically firmer setting and removing the constraint on the magnitude of $\nabla\phi$.

As for the solution of system (50), its mathematical analysis has been attempted by Magnanini and Talenti[61–63], for the case of Hamiltonian (16).

In the framework of extended ray theory[26–31], the first equation of the system is viewed as a Hamilton-Jacobi equation for S, describing orbits of *extended rays* in the real wave phase space (x, N). Extended rays are real-valued (in contrast to complex rays[18–20] that can be "scattered into the complex space") and reduce to the standard geometrical optics rays when $\nabla\phi = 0$. On the other hand, when the imaginary part ϕ of the phase has a non-trivial gradient, Hamilton's equations for extended rays should then be solved together with the partial differential constraint $V(x)\cdot\nabla\phi(x) = 0$, which forces $\nabla\phi$ to be orthogonal to the vector field

$$V(x) = \frac{\partial H}{\partial N}\big(x, \nabla S(x)\big). \tag{51}$$

This is formally the same as the vector field defined in the geometrical optics transport equation (5b), but the analogy is purely formal: the function S here is coupled to ϕ and therefore differs from the corresponding quantity in the standard geometrical optics. This coupling between S and ϕ introduces wave effects.

The vector field (51) should be compared to the velocity field of the bundle of extended rays, which reads

$$V(x) - \frac{1}{2}\frac{\partial\phi}{\partial x^k}\frac{\partial\phi}{\partial x^l}\frac{\partial^3 H}{\partial N\partial N_k\partial N_l}(x, \nabla S).$$

Near the zero-level set $\mathcal{R}$, where $\nabla\phi$ is small, the two vector fields are close one to the other, but differences can be present away from $\mathcal{R}$. In the next section, we shall find that the vector field $V(x)$ represents the wave energy density flux.

Solution of equation (40b). Equation (40a) yields the complex eikonal equation (45a) and the complex polarization condition (45b) exactly in the same form previously derived by heuristics means. There, the advantage of our approach consists just in making the derivation precise and consistent.

For equation (40b), on the contrary, we find significant simplifications with respect to the heuristic approach: removing the unnecessary high-order terms resulted in a simpler dependence of (40b) on the gradient $\nabla\phi$ of the imaginary part of the phase. Such simplifications are pivotal in obtaining the wave energy flux.

On the line of the standard geometrical optics theory, let us first note a necessary condition for the existence of a solution of (40b).

Upon multiplication on the left by the complex extension $\tilde f$ of the dual eigenvector e^*, and noting that

$$\begin{aligned}\tilde f(x,\nabla\psi)\cdot D_0(x,\nabla\psi)a_1(x)\\ = \tilde H(x,\nabla\psi)\tilde f(x,\nabla\psi)\cdot a_1(x) + O(|\nabla\phi|^3),\end{aligned}$$

equation (40b) implies,

$$\begin{aligned}e^*\cdot\Big[&\frac{\partial D_0}{\partial N_i}\frac{\partial\big[A\tilde e(x,\nabla\psi)\big]}{\partial x^i}\\ &+\frac{1}{2}\Big[\frac{\partial^2 D_0}{\partial x^i\partial N_i}+\frac{\partial^2\psi}{\partial x^i\partial x^j}\frac{\partial^2 D_0}{\partial N_i\partial N_j}\Big]eA - i\varepsilon_1 eA\Big]\\ &+O(|\nabla\phi|) = \tilde f(x,\nabla\psi)\cdot\rho_1(x,\nabla\psi),\end{aligned} \tag{52}$$

where all phase space functions, when not explicitly indicated, are assumed to be evaluated at $(x, \nabla S)$, and the notation $\partial[\cdots]/\partial x^k$ denotes the derivative with respect to both the explicit and implicit dependence on x. Here, the term involving the derivative of $\tilde e$ must be dealt with carefully. From definition (41), one gets,

$$\frac{\partial[A\tilde e]}{\partial x^k} = \frac{\partial[Ae]}{\partial x^k} + iA\frac{\partial e}{\partial N_l}\frac{\partial^2\phi}{\partial x^k\partial x^l} + O(|\nabla\phi|),$$

hence,

$$\begin{aligned}e^*\cdot\frac{\partial D_0}{\partial N_k}\frac{\partial[A\tilde e]}{\partial x^k} &= e^*\cdot\frac{\partial D_0}{\partial N_k}\frac{\partial[Ae]}{\partial x^k}\\ &+\frac{iA}{2}e^*\cdot\Big(\frac{\partial D_0}{\partial N_l}\frac{\partial e}{\partial N_k}+\frac{\partial D_0}{\partial N_k}\frac{\partial e}{\partial N_l}\Big)\frac{\partial^2\phi}{\partial x^k\partial x^l}+O(|\nabla\phi|).\end{aligned} \tag{53}$$

The term in round brackets can be computed by making use of the identity obtained by deriving twice the eigenvalue equation $D_0 e = He$ with respect to N, evaluating the result for $N = \nabla S$, and recalling that $H(x, \nabla S) = O(|\nabla\phi|^2)$, in virtue of (50); that reads,

$$\begin{aligned}e^*\cdot\Big(\frac{\partial D_0}{\partial N_l}\frac{\partial e}{\partial N_k}+\frac{\partial D_0}{\partial N_k}\frac{\partial e}{\partial N_l}\Big) &=\\ \frac{\partial^2 H}{\partial N_l\partial N_k} - e^*\cdot\frac{\partial^2 D_0}{\partial N_l\partial N_k}e&\\ +e^*\cdot\Big(\frac{\partial H}{\partial N_l}\frac{\partial e}{\partial N_k}+\frac{\partial H}{\partial N_k}\frac{\partial e}{\partial N_l}\Big)+O(|\nabla\phi|^2).&\end{aligned}$$

After substituting the latter identity into (53), we estimate

$$\frac{\partial H}{\partial N_k}\frac{\partial^2\phi}{\partial x^k\partial x^l} = \frac{\partial V^k}{\partial x^l}\frac{\partial\phi}{\partial x^k} = O(|\nabla\phi|),$$

which follows by applying $\partial/\partial x^l$ to the second equation in (50). Then, (53) becomes

$$\begin{aligned}e^*\cdot\frac{\partial D_0}{\partial N_k}\frac{\partial[A\tilde e]}{\partial x^k} &= e^*\cdot\frac{\partial D_0}{\partial N_k}\frac{\partial[Ae]}{\partial x^k}\\ &+\frac{iA}{2}\Big[\frac{\partial^2 H}{\partial N_l\partial N_k}-e^*\cdot\frac{\partial^2 D_0}{\partial N_l\partial N_k}e\Big]\frac{\partial^2\phi}{\partial x^k\partial x^l}+O(|\nabla\phi|).\end{aligned}$$

and equation (52) reads

$$\begin{aligned}e^*\cdot\frac{\partial D_0}{\partial N_k}\frac{\partial[Ae]}{\partial x^k}+e^*\cdot\Big[\frac{1}{2}\frac{\partial}{\partial x^k}\Big[\frac{\partial D_0}{\partial N_k}\Big]-i\varepsilon_1\Big]eA&\\ +\frac{i}{2}\frac{\partial^2 H}{\partial N_l\partial N_k}\frac{\partial^2\phi}{\partial x^l\partial x^k}A+O(|\nabla\phi|) = \tilde f\cdot\rho_1.&\end{aligned} \tag{54}$$

One can note that the first two terms in equation (54) are formally the same as those in the corresponding equation of standard geometrical optics, which implies the transport equation (5b). The only difference consists in evaluating all phase space functions at $N = \nabla S$, with the pair (S, ϕ) solving system (50); thus, one has $H(x, \nabla S) = O(|\nabla\phi|^2)$ as opposite to the exact local dispersion relation (5a) of the standard geometrical optics. With that in mind, we can follow the lines of the standard theory (cf., for instance Littlejohn and Flynn[36] and references therein), so that,

$$e^* \cdot \frac{\partial D_0}{\partial N_k}\frac{\partial [Ae]}{\partial x^k} + e^* \cdot \left[\frac{1}{2}\frac{\partial}{\partial x^k}\Big[\frac{\partial D_0}{\partial N_k}\Big] - i\varepsilon_1\right] eA$$
$$= \frac{\partial H}{\partial N_k}\frac{\partial A}{\partial x^k} + \left[\frac{1}{2}\frac{\partial}{\partial x^k}\Big[\frac{\partial H}{\partial N_k}\Big] + \gamma_1 - i\delta_1\right] A + O(|\nabla\phi|),$$

where, in particular, the identity (obtained by differentiating the first equation in (50))

$$\frac{\partial H}{\partial x^k} + \frac{\partial^2 S}{\partial x^k \partial x^l}\frac{\partial H}{\partial N_l} = O(|\nabla\phi|),$$

has been accounted for. Thereby, one can see that equation (54) is equivalent to

$$V(x)\cdot\nabla A(x) = \big[-\gamma_1(x) + i\big(\delta_1(x) - \delta_{\text{Gouy}}(x)\big) - \tfrac{1}{2}\nabla\cdot V(x)\big]A(x), \tag{55}$$

where the vector field $V(x)$ is now given by (51), γ_1 and δ_1 are formally the same as in geometrical optics, and, thus, are given by (6) and (7), respectively. In complex eikonal theory, an additional phase shift is found, namely,

$$\delta_{\text{Gouy}}(x) = \frac{1}{2}\frac{\partial^2 H(x,\nabla S)}{\partial N_k \partial N_l}\frac{\partial^2\phi}{\partial x^k \partial x^l}, \tag{56}$$

which is the generalization of the classical Gouy shift[64] and it is entirely due to diffraction effects.

Equation (55) provides the transport equation for the amplitude A, that was left unspecified in equation (45).

Once equation (55) has been solved for the amplitude $A(x)$, one can show that the algebraic equation for a_1 has a solution, by means of an argument analogous to the uniqueness proof for (45), exploiting the completeness and orthogonality relations (47) and (48). As usual, such solution is never computed in practice, hence, we shall not digress in the details.

Statement of the main result. We can now formulate the main result of the foregoing asymptotic construction, and summarize the results of this section.

Let $\psi = S + i\phi$ be a regular solution of the system (50), and let a_0 be amplitude given in (45b), with $A(x)$ a regular solution of the complex geometrical optics transport equation (55). Then, it is possible to find a corrector a_1 such that the complex eikonal wave (31) solves the wave equation (1) for the electric field within an error,

$$|\kappa^{-2}\mathcal{L}(\kappa, x, \nabla)E_{\text{CGO}}(\kappa, x)| \le C\kappa^{-3/2}. \tag{57}$$

As for the case of error estimate (9), this does not provide information on the convergence of E_{CGO} to the exact solution; moreover, it relies on the existence of regular solutions for the complex eikonal ψ and amplitude A: when such solutions break down, estimate (57) fails to be uniform.

On the other hand, the coupling of the real phase S to the imaginary part ϕ successfully removes caustic singularities, at least, for the case of focalized beams, as shown by numerical results[1,26–28,65].

C. Wave energy density flux

One of the advantages of our approach is that the transport equation (55) for the wave amplitude $A(x)$ is obtained in a form which parallels the corresponding transport equation in the standard geometrical optics, cf. equation (5b).

The only additional term in the complex geometrical optics transport equation is the Gouy phase shift, and a phase shift does not affect the transport of $|A|^2$, which reads

$$\nabla\cdot\big[V(x)|A(x)|^2\big] = -2\gamma_1(x, \nabla S)|A(x)|^2. \tag{58}$$

In complex geometrical optics, however, the squared amplitude $|A|^2$ does not account for the whole electric field amplitude as, from (31) and (45),

$$|E_{\text{CGO}}(\kappa, x)|^2 = e^{-2\kappa\phi}|A(x)|^2 + O(1/\sqrt{\kappa}). \tag{59}$$

On the other hand, the orthogonality $V\cdot\nabla\phi = 0$, satisfied by a solution of (50), gives

$$\nabla\cdot\big[V(x)e^{-2\kappa\phi}|A|^2\big] = e^{-2\kappa\phi}\nabla\cdot\big[V(x)|A|^2\big] - 2\kappa e^{-2\kappa\phi}|A|^2 V\cdot\nabla\phi = e^{-2\kappa\phi}\nabla\cdot\big[V(x)|A|^2\big].$$

Upon using this into equation (58), one finds that, formally, the standard geometrical optics energy transport equations (10)-(13) hold true for complex geometrical optics as well, with only one modification in the definition of the wave energy density, namely,

$$W = \frac{1}{16\pi}\left|\frac{\partial(\omega H)}{\partial\omega}\right| e^{-2\kappa\phi}|A|^2, \tag{60}$$

where, we recall, the derivative $\partial/\partial\omega$ should be computed at constant wave vector $k = \omega N/c$. In complex geometrical optics, however, the coefficients of the transport equation (10) should be evaluated at $N = \nabla S$, where now S is the solution of the system (50).

The group velocity, in particular, is

$$v_g = c\left|\frac{\partial(\omega H)}{\partial\omega}\right|^{-1} V(x), \tag{61}$$

with $V(x)$ being the vector field defined in (51). One can conclude that, in complex geometrical optics, the

wave energy density flow is directed along the lines of the vector field $V(x) = \partial H(x, \nabla S)/\partial N$, and this can deviate from the corresponding geometrical optics quantity, due to diffraction effects.

In general, however, the vector field V does not need to be tangent to extended rays; therefore, extended rays, in contrast to standard rays, can fail to represent the energy flow, and one of the most useful features of standard geometrical optics could be missed in complex eikonal theory. Nevertheless, the disagreement between extended rays and the wave energy flow is expected to be small in the region of space where the wave field is localized, cf. comments after equation (51). The differences between extended ray trajectories and the direction of the vector field V are estimated numerically in section IV: typically, they are so small that extended rays can be considered a good approximation of the wave energy flow.

As a cross-check of our results, let us consider the conserved flux naturally implied by equation (1), namely,

$$F(\kappa, x) = \frac{2}{\kappa}\mathrm{Im}\big[E^*(\kappa, x) \times \big(\nabla \times E(\kappa, x)\big)\big]. \qquad (62)$$

Using (1) and (2), one finds

$$\nabla \cdot F = -2E^* \cdot \varepsilon_1^a E,$$

which shows that F is a conserved flux in a non-dissipative medium ($\varepsilon_1^a = 0$). Indeed, F is the normalized Poynting flux, time-averaged over the period $2\pi/\omega$ of the beam (using $E(t, x) = \mathrm{Re}\big\{e^{-i\omega t}E(\kappa, x)\big\}$).

For the specific case of a complex eikonal wave (31) with amplitude given by (45), the flux (62) becomes,

$$F_{\mathrm{CGO}}(\kappa, x) = \big[2\nabla S - (e^* \cdot \nabla S)e - (e \cdot \nabla S)e^*]e^{-2\kappa\phi}|A|^2 + O(1/\sqrt{\kappa}), \qquad (63)$$

where the lowest order has been separated by taking into account estimate (35).

We now need the identity

$$\frac{\partial H}{\partial N_i}(x, \nabla S) = e^*(x, \nabla S) \cdot \frac{\partial D_0(x, \nabla S)}{\partial N_i} e(x, \nabla S) + O(|\nabla\phi|^2),$$

which follows from the derivative of the eigenvalue equation $D_0 e = He$ evaluated at $N = \nabla S$ and multiplied on the left by e^*; the $O(|\nabla\phi|^2)$ remainder stems from the fact that ∇S, with S solution to (50), does not solve exactly the dispersion equation; one has $H(x, \nabla S) = O(|\nabla\phi|^2)$ and $e^* D_0 = He^* = O(|\nabla\phi|^2)$.

When D_0 is given by (3), cf. also equation (37b), the complex geometrical optics flux (63) takes the form

$$F_{\mathrm{CGO}}(\kappa, x) = \frac{\partial H(x, \nabla S)}{\partial N} e^{-2\kappa\phi(x)}|A(x)|^2 + O(1/\sqrt{\kappa}), \qquad (64)$$

showing that the energy flux is proportional to the vector field (51). The leading order term is the transported quantity in equation (58) times the exponential $e^{-2\kappa\phi}$, as discussed above.

The combination of equations (60),(61), and (64) yields the leading order term of the physical Poynting vector, namely,

$$\frac{c}{16\pi}F_{\mathrm{CGO}}(\kappa, x) = v_g(x)W(x) + O(1/\sqrt{\kappa}). \qquad (65)$$

Let us conclude with a remark: although relationship (65) could have been expected on physics basis[31], its derivation does not follow easily by a naive application of the complex eikonal method. Indeed, the paraxial character of complex eikonal waves, introduced in section III A, plays a crucial role in removing unnecessary higher-order terms from the amplitude transport equation. Such a paraxial approach to complex geometrical optics, on the other hand, requires two extra assumptions on both the geometry of the set $\mathcal{R}$ in (33) and the imaginary part ϕ of the complex phase. For instance, should ϕ have been assumed to vanish of second-order on $\mathcal{R}$ (i.e., one additional order with respect to the case considered here), one would have found powers of $\kappa^{-1/3}$, that are the characteristic mark of a fold caustic, cf. section II B. In other words, this approach appears flexible, but requires tuning to the specific caustics geometry.

Our choice, here, has been directed to the description of focused beams, as shown in the numerical examples of the next section.

IV. NUMERICAL RESULTS

In this section, we address numerically a few issues that have not been completely clarified theoretically. First, we shall provide an estimate of differences between the direction of extended rays and that of the field lines of the energy flux vector obtained in section III C for the case of the `GRAY` code[1]. Then, we shall provide a qualitative comparison between extended rays obtained by `GRAY` and the field lines of the energy flux vector, as computed using the the function S from the beam tracing code `TORBEAM`[2]. It is known from previous studies[9,15,31,32] that complex geometrical optics and the paraxial WKB method, upon which `TORBEAM` is based, should give the same results. This also provides a benchmark case of a newly added module in `TORBEAM`, which computes the field lines of $V(x)$ with the aim of both representing the wave energy flow of a beam and allowing a direct coupling of `TORBEAM` to other ray-based codes, like quasi-linear Fokker-Planck solvers. All considered cases refer to a standard ITER plasma equilibrium[66].

A. Extended rays versus energy flux in `GRAY`

The complex geometrical optics code `GRAY` solve equations (50) for the case of the Hamiltonian

$$H(x, N) = N^2 - n^2(x, N_\parallel),$$

the complex extension of which gives the effective Hamiltonian (cf. the first equation of system (50))

$$H_{\text{eff}}(x,N) = N^2 - n^2(x,N_\parallel) - \big|\nabla\phi(x)\big|^2 + \frac{1}{2}\frac{\partial^2 n^2(x,N_\parallel)}{\partial N_\parallel^2}\big(b(x)\cdot\nabla\phi(x)\big)^2, \tag{66}$$

where $n^2(x,N_\parallel)$ is obtained from the Altar-Appleton-Hartree dispersion relation for high-frequency waves in cold magnetized plasmas[34], whereas $N_\parallel = b(x)\cdot N$ is the real parallel refractive index, with $b(x)$ the unit vector of the local equilibrium magnetic field.

The function (66) is used as a Hamiltonian in the (x,N) phase space, while ϕ is computed from the partial differential equation $V\cdot\nabla\phi = 0$, which, in particular, gives the imaginary part $N' = \nabla\phi$ of the refractive index. The resulting Hamiltonian orbits projected into the configuration space give extended rays.

At each grid point $x = (\mathsf{x},\mathsf{y},\mathsf{z})$ along extended rays, both the vector $T(x)$, tangent to the ray, and the vector $V(x)$, cf. equation (51), proportional to the energy flux, are evaluated, and the angle ϑ spanned by the two is computed according to

$$T(x)\cdot V(x) = |T(x)||V(x)|\cos\vartheta. \tag{67}$$

Figures 2 and 3 show the results for four cases of electron cyclotron beams, launched from the equatorial plane in ITER (the exact launching position is the same in all cases: x = 930cm, y = 0cm, and z = 70cm). In figure 2, the beam has a mild focalization similar to ITER operational parameters, i.e., the equivalent focal length in free space is z_f = 200cm with an equivalent waist w_0 = 2cm, and the beams are launched at poloidal angle $\alpha = 0°$ and different toroidal angles, namely, $\beta = 0°$ (upper panels), $\beta = 20°$ (middle panels), and $\beta = 40°$ (lower panels). In figure 3, the results for a beam with high focalization are displayed; in this case, the equivalent focal length in free space is z_f = 150cm, with the equivalent waist w_0 = 0.5cm, poloidal injection angle $\alpha = 0°$, and toroidal injection angle $\beta = 0°$. Such a highly focused beam largely exceeds ITER parameters, but it has been considered as an example in which the effects of diffraction are emphasized.

On the left-hand side of figures 2 and 3, the initial positions of extended rays projected in the y-z plane are shown. One can see that rays are launched from a polar grid of points; the electric field amplitude is a Gaussian with the maximum at the center of the ray bundle, and points at the same radial position lie on the same amplitude level contour. For this test a large number of rays is considered, so that the beam is covered up to the $1/e^4$-level of its amplitude: this is a much larger beam section than usually needed. Each point is represented in a gray scale, which encodes the maximum value of the angular deviation $1-\cos\vartheta$, with ϑ given in (67), observed along the ray issued from that point. The approximate direction of the local magnetic field in the low-field side projected onto the y-z plane is indicated by an arrow (this is approximated by the value of the numerical equilibrium magnetic field at the nearest grid node to the launching point, specifically, at major radius coordinate R = 850.0cm and vertical coordinate z = 70.3125cm of the numerical grid). The distribution of angular deviations allows us to appreciate geometric effects: in all considered cases, rays for which the angular deviation attains its maximum are those aligned to the magnetic field. This can be understood by inspection of the effective Hamiltonian (66). The difference between the ray and the energy flow directions is proportional to the product $N_\parallel(N_\parallel')^2$ of the real parallel refractive index and the square of the imaginary parallel refractive index $N_\parallel' = b(x)\cdot\nabla\phi(x)$; the factor $N_\parallel$ is obtained on noting that, for the Altar-Appleton-Hartree dispersion relation, the third-order derivative of n^2, cf. comments after equation (51), is proportional to $N_\parallel$, while the factor $(N_\parallel')^2$ comes from the complex extension. It follows that rays with a large $N_\parallel$ show larger deviations.

For each case of figures 2 and 3, we have selected the "worst ray", i.e., the ray for which the maximum angular deviation is observed, and the corresponding profile of $1-\cos\vartheta$ is plotted as a function of the arc-length s along the central ray (which is used as a common parameter for all rays). The profiles of both the real and imaginary parts of the parallel refractive index, as well as the profiles of the two beam widths are also reported for a comparison. One can see that the maximum deviation occurs, as expected, near the waist of the beam, where diffraction effects are more important, and, thus, the imaginary part of the refractive index increases. For the cases of exactly perpendicular injection (toroidal angle $\beta = 0°$), a double-peak structure of the deviation profile is observed: the local minimum is found where $N_\parallel$ is zero, which implies that the difference between the ray flow and the energy flow must vanish. In passing, let us mention that the slight discontinuity in the profiles of both the real and imaginary parallel refractive indices is due to the way the equilibrium magnetic field has been extended outside the grid of the numerical equilibrium: there, the propagation happens in free space, and the precise value of the magnetic field is unimportant; for the calculation of parallel refractive indices, a rough approximation is used, and that does not match continuously to the numerical equilibrium at the boundary of the grid.

The overall conclusion from figure 2 is that, under ITER-relevant conditions, deviations of extended rays from the energy flow are small, even for large toroidal injection angles, which should increase $N_\parallel$. The same is found for the highly focused beam of figure 3, for which diffraction effects should be stronger. It is, therefore, possible to approximate the energy flow of the beam by the extended ray flow.

The reason for such a good agreement is that the physically interesting domain, where rays are traced in practical applications, coincides with a neighborhood of the zero level curve $\mathcal{R}$ of the imaginary phase ϕ, cf. equation

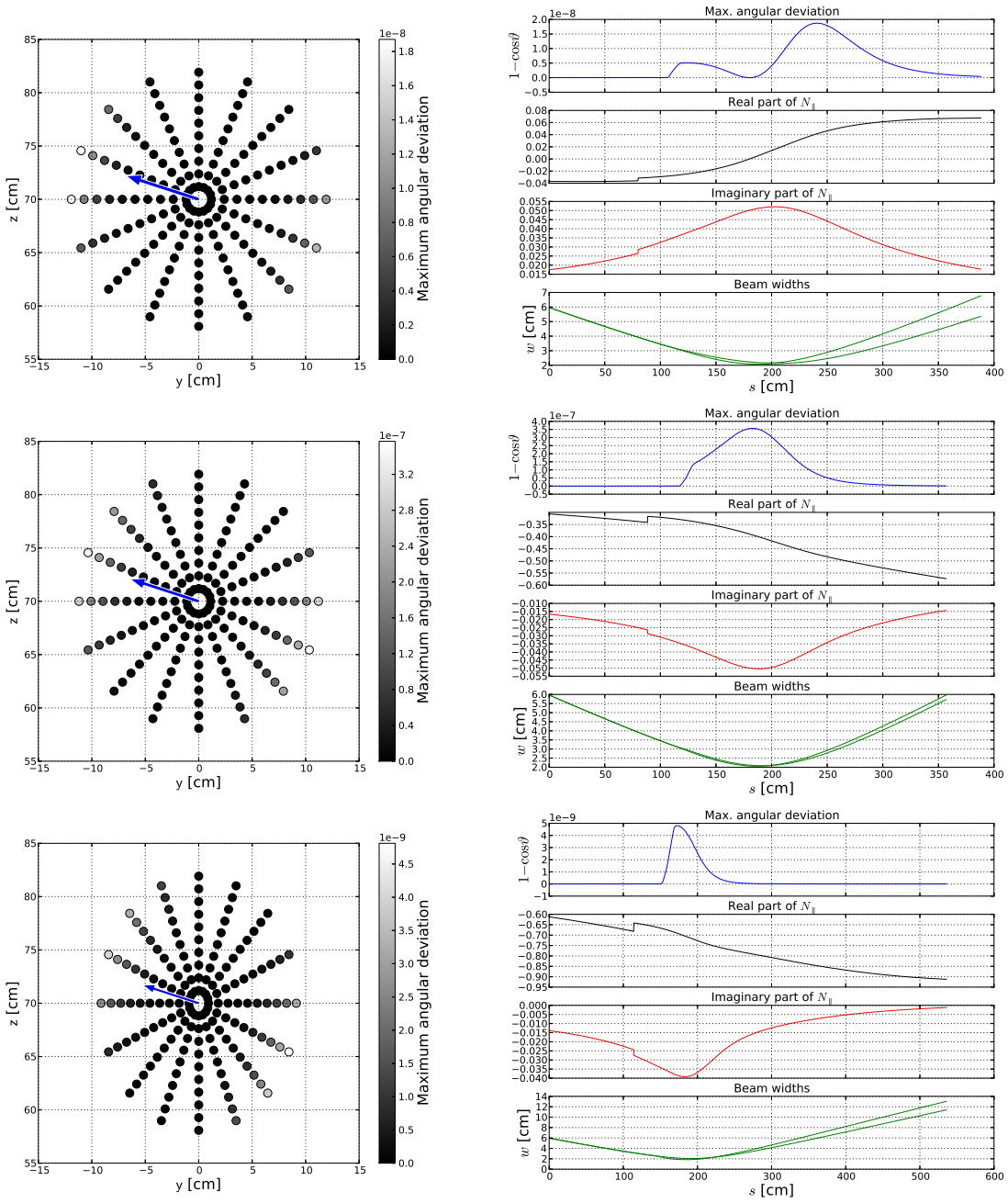

FIG. 2. Angular deviation $1-\cos\vartheta$ of extended rays, cf. equation (67), as computed by the GRAY code. Left-hand side plots show the initial positions of extended rays, projected on the y-z plane; the gray level of each point encodes the maximum deviation observed along the corresponding ray, and the approximate direction of the equilibrium magnetic field is indicated by an arrow. Right-hand side plots show the profile of the deviation for the "worst ray", compared to both the real and imaginary parts of the parallel refractive index, as well as to the two beam widths. In all cases, the equivalent focal length and waist are $z_f = 200$cm and $w_0 = 2$cm, respectively; the poloidal injection angle is $\alpha = 0°$, and the toroidal injection angles are $\beta = 0°$ (upper panels), $\beta = 20°$ (middle panels), and $\beta = 40°$ (lower panels).

(33); there, the gradient $\nabla\phi$ is close to zero (it vanishes identically on $\mathcal{R}$, cf. section III A), and the second term in the Hamilton-Jacobi equation (50) act as a small perturbation.

B. Extended rays versus paraxial WKB energy flux

The transport equation (58) is exactly the same as the energy transport equation obtained in the framework of the paraxial WKB approach[8,9]. Furthermore, equation (50), Taylor-expanded around the curve $\mathcal{R}$, yields the

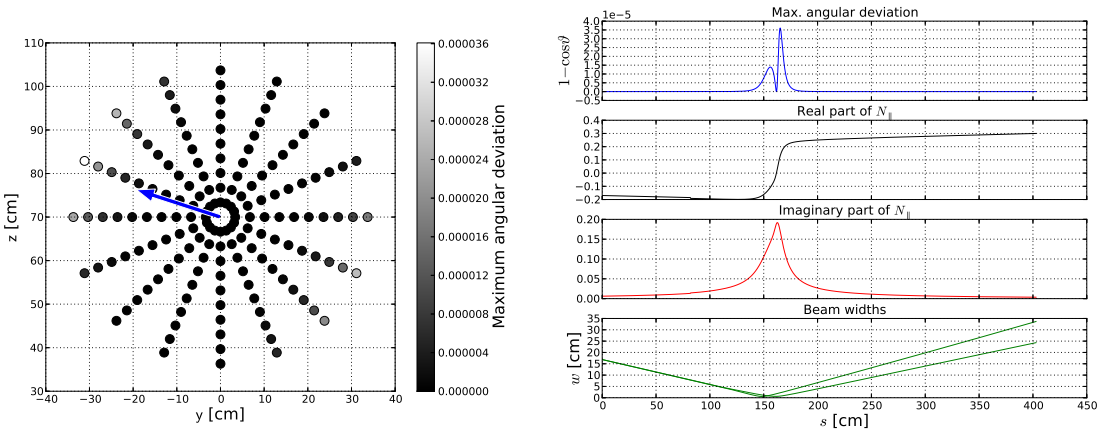

FIG. 3. The same as in figure 2, but for $z_f = 150$cm, $w_0 = 0.5$cm, $\alpha = 0°$, and $\beta = 0°$.

matrix Riccati equation for the Hessian of the phase of the paraxial WKB method[15,31,32]. It is therefore natural to compare the results of the complex geometrical optics code GRAY[1] with those of the paraxial WKB code TORBEAM[2]. This is made possible by a newly implemented module in TORBEAM, which solves the set of ordinary differential equations

$$\frac{dx}{d\tau} = V(x), \tag{68}$$

where $V(x)$ is defined by (51), with the real phase S being here computed in the paraxial WKB framework. The result is a bundle of curves which represents the energy flow of the beam.

Figure 4 shows a qualitative comparison between the extended rays computed by GRAY and the TORBEAM solution of equation (68) with initial conditions given by the initial position of GRAY rays; we refer to the latter as TORBEAM rays, for simplicity. The case considered is the same as in figure 2, upper panels: the focusing is typical for ITER parameters. On looking at the three-dimensional position of the beam (shown on the right-hand side plot, with respect to the ITER last magnetic surface), one can note the rather long propagation path of the beam; it is also apparent that the y-z plane is roughly orthogonal to the beam axis. It is, therefore, convenient to project both GRAY and TORBEAM rays on the y-z plane; the result is shown on the left-hand side plot for the rays corresponding to the $1/e^2$-level of the amplitude only. The common initial positions of rays are marked by dots; starting from those marked points both GRAY and TORBEAM rays propagate inward, reach the waist and then turn outward. One can see that TORBEAM and GRAY rays are in good agreement. Indeed, for the inward part of the propagation, up to the waist, GRAY and TORBEAM rays are superposed within the resolution of the plot. They start deviating one from the other near the waist. However, such deviations are quantitatively small: considering the differences in the numerical schemes of the two codes and the different treatment of the plasma-vacuum interface, as well as the long propagation path, such an agreement appears satisfactory.

This comparison has been repeated for the highly focused case of figure 3 and the results are displayed in Figure 5. Now the differences are one order of magnitude larger than in the case of figure 4, but the beam cross-section has also increased by one order of magnitude.

The foregoing numerical experiment, in addition, illustrates how the information on extended rays is actually encoded in the paraxial WKB solution as well, despite the paraxial approach describes the wave beam through a set of parameters on a *single ray*, i.e., the central ray.

V. ACCOUNTING FOR SPATIAL DISPERSION

The theory reported in section III is by no means limited to the case of a spatially non-dispersive media as far as the condition (2) of the dielectric tensor (which in general depends on both (x, N)) is satisfied.

From the point of view of the description of electron cyclotron wave beams in tokamak physics, spatial dispersion is found as a consequence of temperature effects in the response of the plasma[33] and might be a concern for high temperature devices. However, it is believed that the cold plasma approximation is valid up to the region where the beam is absorbed by resonating electrons. There, temperature effects and, thus, spatial dispersion, cannot be neglected, but in such situation condition (2) is violated, thus, turning such a dispersive generalization of complex geometrical optics into a mere theoretical exercise.

Nonetheless, from the point of view of the theory of the complex geometrical optics, the issue of the generalization appears interesting. We give here a sketch of the derivation only.

The basic idea is to take advantage of the pseudodifferential form the the wave equation for a generic dispersive stationary medium[6]. Specifically, the wave electric field

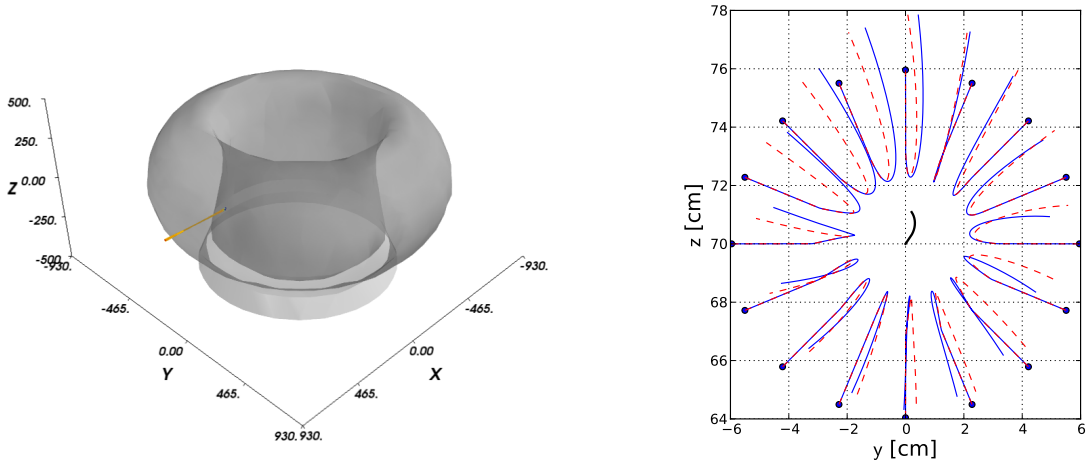

FIG. 4. Visualization of extended rays for the case $z_f = 200$cm, $w_0 = 2$cm, and $\alpha = \beta = 0°$ of figure 2. The three-dimensional position of the beam with respect to the ITER last magnetic surface (left hand side plot) shows the physical proportions of the beam, and the rather long propagation path (~ 400cm). The projection of rays on the y-z plane (right-hand side plot) shows the differences between `GRAY` rays (dashed, red, curves) and `TORBEAM` rays (solid, blue, curves). The central ray is also shown (thick, black, curve) at the center of the beam.

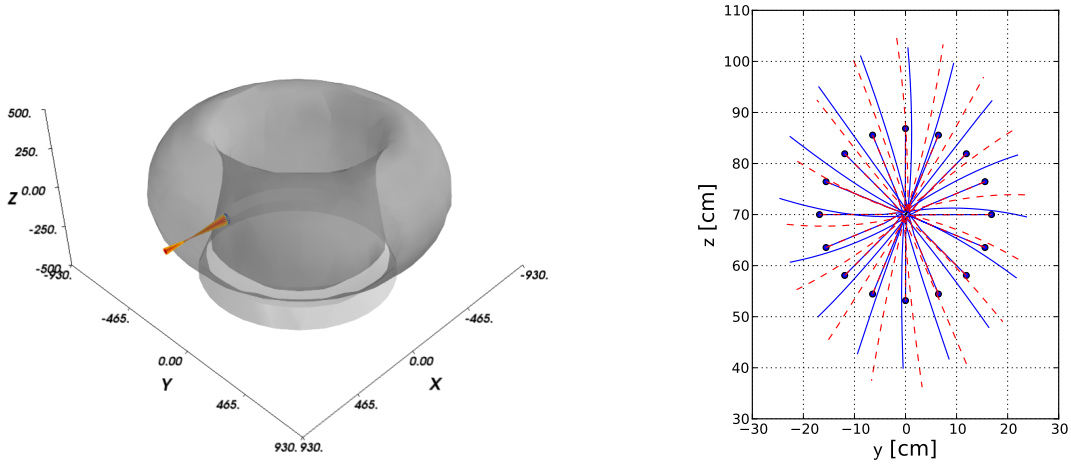

FIG. 5. The same as in figure 4, but for the highly focused case: $z_f = 150$cm, $w_0 = 0.5$cm, $\alpha = \beta = 0°$.

satisfy an integral equation, which can be written in the form

$$D^w(\kappa, x, -\tfrac{i}{\kappa}\nabla)E(\kappa, x) = \left(\frac{\kappa}{2\pi}\right)^d \times \int e^{i\kappa(x-x')\cdot N} D(\kappa, \tfrac{x+x'}{2}, N)E(\kappa, x')dx'dN = 0, \tag{69}$$

where

$$D_{ij}(\kappa, x, N) = N^2\delta_{ij} - N_iN_j - \varepsilon_{ij}(\kappa, x, N),$$

is the Weyl symbol[6,35] of the semiclassical pseudodifferential operator $D^w(\kappa, x, -(i/\kappa)\nabla)$, $1/\kappa$ being the semiclassical parameter.

Assuming the equivalent of condition (2), one has

$$D(\kappa, x, N) = D_0(x, N) + \frac{1}{\kappa}D_1 + \cdots,$$

where the leading order term (i.e., the semiclassical principal symbol[35]) is Hermitian. Exactly as in the non-dispersive case, we assume that the (real) eigenvalues of D_0 are well separated, as discussed in section II A, so that we do not have to be worried about linear mode conversion.

Let us start deriving a useful asymptotic form of the wave equation. We consider the electric field in the form

$$E(\kappa, x) = e^{i\kappa S(x)}w(\kappa, x), \tag{70a}$$

where the amplitude $w(\kappa, x)$ is allowed to have fast variations, namely,

$$\left|\partial_x^\alpha w(\kappa, x)\right| \leq C\kappa^{r|\alpha|}, \tag{70b}$$

in the limit $\kappa \to +\infty$, where C is a constant depending only on the multi-index $\alpha = (\alpha_1, \ldots, \alpha_d)$, and r is a fixed real parameter with $0 \leq r < 1$; each derivative increase the order by a factor κ^r. The fast variations of the amplitude distinguish the wave field (70) from the standard (real) eikonal wave (8).

The complex eikonal wave (31) have the form (70), with

$$w(\kappa, x) = e^{-\kappa\phi(x)} a(\kappa, x), \tag{71}$$

and $r = 1/2$, provided that the two conditions on the paraxial field, cf. section III A, are fulfilled. This follows from estimate (35), which allows us to control the derivative,

$$|\nabla\big(e^{-\kappa\phi(x)}a(\kappa,x)\big)| \leq \kappa C|\nabla\phi e^{-\kappa\phi(x)}a(\kappa,x)| = O(\sqrt{\kappa}).$$

The substitution of the field (70) into the wave equation (69), along with lengthy but standard calculations[6], yields,

$$\begin{aligned}&\frac{i}{\kappa}\frac{\partial D_0}{\partial N_k}\frac{\partial w}{\partial x^k} + \frac{1}{2\kappa^2}\frac{\partial^2 D_0}{\partial N_k \partial N_l}\frac{\partial^2 w}{\partial x^k \partial x^l} \\ &- \left[D_0 - \frac{i}{2\kappa}\Big(\frac{\partial}{\partial x^k}\Big[\frac{\partial D_0}{\partial N_k}\Big] + 2iD_1\Big)\right] w + O(\kappa^{-3/2}) = 0,\end{aligned} \tag{72}$$

where the case $r = 1/2$ has been considered. One can now substitute the form (71) specific to complex eikonal waves, with the amplitude given by (31b) and, collecting terms, one has

$$\begin{aligned}&e^{i\kappa\psi}\Bigg\{\tilde{D}_0(x, \nabla\psi)a_0(x) \\ &\quad + \frac{1}{\kappa}\Bigg[D_0(x,\nabla S)a_1 - i\Big[\frac{\partial D_0}{\partial N_i}(x,\nabla S)\frac{\partial a_0}{\partial x^i} \\ &\quad + \frac{1}{2}\Big[\frac{\partial^2 D_0}{\partial x^i \partial N_i}(x,\nabla S) + \frac{\partial^2\psi}{\partial x^i \partial x^j}\frac{\partial^2 D_0}{\partial N_i \partial N_j}(x,\nabla S)\Big]a_0 \\ &\quad + iD_1 a_0\Big]\Bigg]\Bigg\} + O(\kappa^{-3/2}) = 0,\end{aligned} \tag{73}$$

where $\psi = S + i\phi$, and

$$\begin{aligned}\tilde{D}_0(x,\tilde{N}) &= D_0(x,N) \\ &\quad + i\frac{\partial D_0(x,N)}{\partial N_k}N'_k - \frac{1}{2}\frac{\partial^2 D_0}{\partial N_k \partial N_l}N'_k N'_l.\end{aligned}$$

Equation (73) (except for an overall factor κ^2) is formally the same as equation (39), with the only difference that the complex extension $\tilde{D}_0$ needs to be considered, with the dispersion tensor D_0 given by the principal part of the Weyl symbol in (69); moreover, $-\varepsilon_1$ is replaced by D_1. Particularly, the complex extension $\tilde{D}_0$ is found here naturally in the very same form as that used in the solution of equation (40a) of section III.

With such replacements being implied, we can conclude that the results on the complex geometrical optics solution are also valid for dispersive media. Let us also remark that this approach does not exploit the specific form of the symbol $D(\kappa, x, N)$. The results are, therefore, valid for a broader class of wave equations, i.e., semiclassical pseudodifferential wave equations having a sufficiently regular symbol with a Hermitian principal part.

ACKNOWLEDGMENTS

Many ideas, upon which we have strongly relied in developing our arguments, are Grigory Pereverzev's. His keen insights and guidance are deeply missed.

O. M. wish to thank Marino Bornatici and Roberto Pozzoli for many discussions, constructive criticisms, and tutorship during his Ph. D. work, which, in part, has been used here. A. M. wish to thank Roberto Pozzoli for the tutorship during his Master's degree and Ph. D. work on this subject and Lorenzo Figini for the help with the `GRAY` code.

[1] D. Farina, Fusion Sci. Technol. **52**, 154 (2007).
[2] E. Poli, A. G. Peeters and G. V. Pereverzev, Comp. Phys. Comm. **136**, 90 (2001).
[3] R. Prater, Nucl. Fusion **48**, 035006 (2008).
[4] V. M. Babič and V. S. Buldyrev, *Short-Wavelength Diffraction Theory*, Springer-Verlag (Berlin 1991).
[5] Yu. A. Kravtsov and Yu. I. Orlov, *Geometrical Optics of Inhomogeneous Media*, Springer (Berlin 1990).
[6] S. W. McDonald, Phys. Rep. **158**, 337-416 (1988).
[7] J. Rauch, *Lectures on geometric optics*, IAS-Park City Math. Ser. 5, AMS (Providence, RI, 1998).
[8] G. V. Pereverzev, in *Reviews of Plasma Physics*, Vol. 19, edited by B. B. Kadomtsev, Consultants Bureau (New York, 1996) .
[9] G. V. Pereverzev, Phys. Plasmas **5**, 3529 (1998).
[10] V. P. Maslov, *The Complex WKB Method for Nonlinear Equations I: Linear Theory*, Birkhäuser (Basel, 1994).
[11] M. M. Popov, *Ray Theory and Gaussian Beam Method for Geophysicists*, EDUFBA (Salvador-Bahia, 2002).
[12] M. Motamed and O. Runborg, Wave Motion **47**, 421 (2010).
[13] G. Ariel, B. Engquist, N. M. Tanushev and R. Tsai, J. Comp. Phys. **230** 2303 (2011).
[14] E. Heyman and L. B. Felsen, J. Opt. Soc. Am. A **18**, 1588 (2001).
[15] M. Bornatici and O. Maj, Plasma Phys. Control. Fusion **45**, 707 (2003).
[16] Yu. A. Kravtsov, *Geometrical Optics in Engineering Physics*, Alpha Science (Harrow, UK, 2005).
[17] V. Černevý, *Seismic Ray Theory*, Cambridge U. Press (Cambridge, 2001).
[18] Yu. A. Kravtsov, G. W. Forbes and A. A. Asatryan, in Progress in Optics, E. Wolf ed., Elsevier (Amsterdam, 1999), Vol. XXXIX, pp. 162.
[19] C. J. Thomson, Stud. Geophys. Geod. **41**, 345 (1997).
[20] S. J. Chapman, J. M. H. Lawry, J. R. Ockendon and R. H. Tew, SIAM Review **41**,417 (1999).
[21] R. A. Egorchenkov and Yu. A. Kravtsov, J. Opt. Soc. Am. A **18**, 650 (2001).
[22] D. Amodei, H. Keers, D. Vasco and L. Johnson, Phys. Rev. E **73**, 036704 (2006).
[23] A. Bravo-Ortega and A. H. Glasser, Phys. Fluids B **3**, 529 (1991).

[24]A. Cardinali, Proceedings of the 14th International Conference on Radio Frequency Power in Plasmas, Oxnard, California, 2001, p. 166.
[25]A. Cardinali, Proceedings of the International School of Plasma Physics Piero Caldirola, Theory of Fusion Plasmas, Varenna, Italy, Aug. 2000, p. 439.
[26]S. Choudhary and L. B. Felsen, IEEE Trans. Antennas Propag. **AP-21**, 827 (1973).
[27]E. Mazzucato, Phys. Fluids B **1**, 1855 (1989).
[28]S. Nowak and A. Orefice, Phys. Fluids B **5**, 1945 (1993).
[29]S. Nowak and A. Orefice, Phys. Plasmas **1**, 1242 (1994).
[30]S. Nowak and A. Orefice, J. Plasma Physics **57**, 349 (1997).
[31]A. G. Peeters, Phys. Plasmas **3**, 4386 (1996).
[32]A. V. Timofeev, Physics-Uspeki **48**, 609 (2005).
[33]M. Bornatici, R. Cano, O. De Barbieri and F. Engelmann, Nucl. Fusion **23**, 1153 (1983).
[34]D. B. Melrose and R. C. McPhedran, *Electromagnetic processes in dispersive media*, Cambridge U. Press (Cambridge, 1991).
[35]A. Martinéz, *An Introduction to Semiclassical and Microlocal Analysis*, Springer-Verlag (New York, 2002).
[36]R. G. Littlejohn and W. G. Flynn, Phys. Rev. A **44**, 5239 (1991).
[37]C. Emmrich and A. Weinstein, Comm. Math. Phys. **176**, 701 (1996).
[38]M. E. Taylor, *Partial Differential Equations I: Basic Theory*, 2nd edition, Springer (New York, 2011).
[39]L. Hörmander, *The Analysis of Linear Partial Differential Operators III*, Springer (Berlin, 1985). Chapter 21.
[40]J. J. Duistermaat, *Fourier Integral Operators*, Progress in mathematics, Birkhäuser (Boston, 1996).
[41]J. J. Duistermaat, Comm. Pure Appl. Math. **27**, 207 (1974).
[42]L. Hörmander, *The Analysis of Linear Partial Differential Operators IV*, Springer (Berlin, 1985).
[43]V. Guillemin and S. Sternberg, *Geometric Asymptotics*, Mathematical Surveys N. 14, AMS (Providence, 1977).
[44]E. De Micheli and G. A. Viano, Applicable Analysis **85**, 181 (2006).
[45]D. Ludwig, Comm. Pure Appl. Math. **19**, 215 (1966).
[46]Yu. A. Kravtsov and Yu. I. Orlov, *Caustics, Catastrophes and Wave Fields*, Springer (Berlin 1993).
[47]J. F. Nye, *Natural focusing and the fine structure of light*, IoP Publishing (Bristol, 1999).
[48]A. H. Glasser and A. Bravo-Ortega, Phys. Fluids **30**, 797 (1987).
[49]Yu. A. Kravtsov and Yu. I. Orlov, Sov. Phys. Usp. **23**, 750 (1980).
[50]E. R. Tracy, A. J. Brizard, D. Johnston, A. N. Kaufman, A. S. Richardson, N. Zobin, Commun. Nonlinear Sci. Numer. Simulat. **17**, 2161 (2012).
[51]L. Hörmander, *Lectures on Nonlinear Hyperbolic Differential Equations*, Springer (Berlin, 1997).
[52]O. Runborg, Comm. Comput. Phys. **2**, 827 (2007).
[53]J.-D. Benamou, Journal of Scientific Computing **19**, 63 (2003).
[54]V. P. Maslov and M. V. Fedoriuk, *Semi-classical approximation in quantum mechanics*, Translated from Russian, D. Reidel Pub. (Dordrecht, Holland, 1981).
[55]S. Hansen and D. Röhrig, Math. Nachr. **277**, 47 (2004).
[56]J. J. Duistermaat, *Stationary Phase Approximation*, in Encyclopedia of Mathematical Physics, Academic Press (Oxford, 2006), Pages 44-49.
[57]A. S. Richardson, P. T. Bonoli and J. C. Wright, Phys. Plasmas **17**, 052107 (2010).
[58]R. A. Cairns and V. Fuchs, Nucl. Fusion **50**, 095001 (2010).
[59]V. L. Ginzburg, in Propagation of Electromagnetic Waves in Plasma, Translated from the Russian by Royer and Roger, edited by W. L. Sadowski, Gordon and Breach, (New York, 1961).
[60]O. Maj, *Complex geometric optics for symmetric hyperbolic systems I: linear theory*, arXiv:0802.1691v1 [math-ph], section 3.
[61]R. Magnanini and G. Talenti, Contemporary Mathematics **283**, 203 (1999).
[62]R. Magnanini and G. Talenti, SIAM Journal on Mathematical Analysis **34**, 805 (2002).
[63]R. Magnanini and G. Talenti, Applicable Analysis **85**, 249 (2006).
[64]M. Born and E. Wolf, *Principles of Optics*, Pergamon (Oxford, 1980), pp. 447, 448.
[65]E. Poli, G. V. Pereverzev, A. G. Peeters and M. Bornatici, Fusion Engineering and Design **53**, 9 (2001).
[66]G. Ramponi, D. Farina, M. A. Henderson, E. Poli, O. Sauter, G. Saibene, H. Zohm and C. Zucca, Nucl. Fusion **48**, 054012 (2008).